GEOLOGICAL SURVEY OF FINLAND
Industrial Environment and Recycling
Kuopio

30.04.2018 GTK/219/03.01/2016

Prediction of the Drainage Water Quality from Mine Wastes with Reactive Transport Modelling

Muhammad Muniruzzaman, Teemu Karlsson & Päivi M. Kauppila

GTK Open File Work Report 12/2018

GEOLOGICAL SURVEY OF FINLAND **DOCUMENTATION PAGE**

30.04.2018 / GTK/219/03.01/2016

Authors
Muhammad Muniruzzaman, Teemu Karlsson and Päivi Kauppila

Type of report
GTK Open File Work Report

Comission by
Mining waste management methods project (KaiHaMe); EU ERDF

Title of report
Prediction of the Drainage Water Quality from Mine Wastes with Reactive Transport Modelling

Abstract
This work presents a predictive model that can be used at the early phase of a mine when data is very limited. The model formulation is based on the reactive transport modelling approaches by taking into account water flow, gas transport and mineral weathering reactions. Furthermore, this report also includes example case studies (both in waste rock pile and tailings systems) demonstrating the scope and capability of the presented model and how such approaches can be effectively attempted especially in potential future sites.

Keywords
Predictive modelling, reactive transport modelling, drainage quality, AMD, simulation

Geographical area
Finland

Map sheet

Other information

Report serial
GTK Open File Work Report 12/2018

Archive code

Total pages
67

Language
English

Price
0 €

Confidentiality
Public

Unit and section
Industrial Environment and Recycling

Project code
KaiHaMe 50403-300432

Siganture/name
Muhammad Muniruzzaman
Research Scientist

Signature/name
Antti Pasanen
Senior Scientist

Contents

Documentation page

1 INTRODUCTION

Management of mine wastes is a prescient issue in mining sectors since uncontrolled waste disposal may result in liability for the operators with the risk of severe financial consequences as well as reputational damage (e.g. Blowes et al. 2014). Of primary concern is the release of toxic drainage from the waste deposits that leads to harmful effects on the environment, ecosystem, and human health (e.g. Blowes et al. 2014, Nordstrom et al. 2015). Such polluted drainages are known to be produced from the weathering of sulphide-rich waste deposits under oxic environments and/or under the influence of microbial activities (e.g. Blowes & Ptacek 1994, Tremblay & Hogan 2000, Amos et al. 2015, Nordstrom et al. 2015). Depending on the mineralogical assemblages and involved key processes, these weathering mechanisms may lead to acidic, circumneutral, or saline drainages (e.g. Nordstrom et al. 2000, Blowes et al. 2014). Although, the acidic drainage is often referred as the most hazardous condition in such environments, the other non-acidic forms of drainages also have the similar potential to release severely contaminated substances to the environment. Therefore, it is of utmost importance to understand the controlling physicochemical processes leading to toxic drainage in mining environments to sufficiently predict the overall system behaviour. Prior understanding about the broadcast of possible future series of events in waste dumps may help achieving a better control on the overall risk assessment, prevention of environmental pollution, and implementation of effective remediation measures (e.g. Dold 2017).

In the past, mine waste drainage problem has received a great deal of attention from mining industries, governmental authorities, and scientists (e.g. Parbhakar-Fox & Lottermoser 2015). In fact, extensive research efforts have been devoted to understand, accurately describe, and predict relevant processes controlling the generation and release of contaminated drainage from mine wastes (e.g. Tremblay & Hogan 2000, Nordstrom et al. 2015). As a result, a plethora of prediction techniques have been developed including experimental methods based on laboratory and field scale tests to characterize different properties of waste materials (e.g. Morin & Hutt 1994, Price 2009, Dold 2017), as well as numerical modelling approaches to quantitatively describe the system dynamics capturing all the key processes (e.g. Mayer et al. 2003, Maest et al. 2005, Amos et al. 2015). In the last few decades, textbooks, general reviews, and guidelines have been published focusing on the context of overall mine waste management (e.g. Morin & Hutt 1994, White et al. 1994, 1999, Nordstrom & Alpers, 1999, Plumlee 1999, Blowes et al. 2003, 2007, INAP 2009, Lottermoser 2010, Kauppila et al. 2013, Dold 2017, MEND 2017), characterization of the acidic drainage generation processes and the properties of the waste deposits (e.g. Bigham & Nordstrom 2000, Rimstidt & Vaughan 2003, Sapsford et al. 2007, Amos et al. 2015, Parbhakar-Fox & Lottermoser 2015, Muniruzzaman et al. 2018), or implementation of different remediation methods (e.g. Johnson & Hallberg 2005, Akcil & Koldas 2006, Tripathy 2014). The common predictive tools available today include a wide range of laboratory and field tests such as mineralogical analysis and physical properties characterization (e.g. Reynolds 1989, Jambor 2003, Williams & Diehl 2014, Declercq et al. 2017), geochemical rock analysis (e.g. Crock et al. 1999, Briggs & Maier 2002, Dold 2003), static tests and chemical extractions on waste deposit samples (e.g. Sobek et al. 1978, Miller et al. 1990, Lawrence & Wang 1997, Price 1997, Morin & Hutt 1999, Heikkinen & Räisänen

2008, 2009, AMIRA 2002, Dold 2003), and kinetic tests (e.g. Hansen et al. 2000, INAP 2009, Price 2009, MEND 2012, ASTM 2013, and Maest & Nordstrom 2017). Additionally, numerical modelling has been proved to be an invaluable tool not only to quantitatively describe the controlling processes leading to the release of acidic/contaminated drainage in mining environments but also to predict the occurrence of future series of events in waste dump systems by explicitly resolving the coupled geochemical and physical mechanisms (e.g. Mayer et al. 2003, Maest et al. 2005, Blowes et al. 2014, Amos et al. 2015, Mayer et al. 2015 Pedretti et al. 2017).

Numerical modelling has been extensively used in investigations related to prediction and quantification of the effects of physical and geochemical processes on the ultimate effluent qualities from the mine waste dumps (e.g. Mayer et al. 2003, Steefel et al. 2005, Blowes et al. 2014, Amost et al. 2015). Basic philosophy of such predictive modelling approaches stems from the concept of the fundamental laws of first principles by comprehensively coupling the computational fluid mechanics with the detailed geochemistry and heat transfer mechanisms (e.g. Barry et al. 2002, Steefel et al. 2015). In the simulations concerning mine wastes, a wide variety of modelling tools has been applied in the literature with the formulations based on both the empirical and mechanistic approaches (e.g. Mayer et al. 2003, Maest et al. 2005). However, for strictly predictive purposes, empirical formulations are not suitable as they lack the necessary theoretical basis, hence, the mechanistic approaches are necessary in order to predict the system dynamics within a particular waste dump (e.g. Nordstrom & Munoz 1994, Maest et al. 2005). Depending on the capabilities, these predictive models are usually categorized as geochemical models that take into account only the geochemical processes occurring in the waste piles (e.g. Parkhurst et al. 1985, Davies & Ashenberg 1987, Ball et al. 1987, Blowes & Jambor 1990, Allison et al. 1991, Wolery et al. 1992, Alpers & Nordstrom 1999, Tempel et al. 2000, Eary et al. 2003, Ramstedt et al. 2003, Moncur et al. 2005, Gunsinger et al. 2006, Nordstrom & Campbell 2014), and more sophisticated reactive transport models that are capable to simultaneously capture hydrogeological processes, multicomponent solute and gas transport processes, thermal processes, microbiological and electrochemical mechanisms in addition to the geochemical processes (e.g. Pantelis 1993, Steefel & Lasaga 1994, Wunderly et al. 1996, Bethke 1997, Mayer et al. 2002, Parkhurst et al. 2005, da Silva et al. 2009, Amos et al. 2015, Nordstrom & Nicholson 2017). Notable examples regarding the rigorous applications of numerical simulations in mining environments include but not limited to Eriksson & Destuoni (1997), Lefebvre et al. (2001), Mayer et al. (2002), Fala et al. (2005, 2013), Linklater et al. (2005), Molson et al. (2005), da Silva et al. (2009), Javadi et al. (2012), Lahmira & Lefebvre (2014), Lahmira et al. (2016), Shokri et al. (2016), Pabst et al. (2017), and Pedretti et al. (2017). However, published studies based on the systematic predictive modelling in a potential future (i.e. planned/proposed) waste facility at the early planning phase of a mine (i.e. prior to the initiation of full scale mining operations and before the construction of the actual waste pile) are scarce in the literature (e.g. Charles et al. 2016) even though the assessment of long-term predictions on seepage chemistry at such initial stage would certainly facilitate a better planning for the waste management. Possible reasons for such lacking in the early stage rigorous analyses might be associated with the unavailability of good quality data that are essential to build realistic site-specific conceptual models, as well as simply due to the lack of

attention on the systematic numerical simulations at such early risk assessment procedures. Another possible reason may include the general lack of interest in publishing the results by the risk assessment conducting parties (i.e. especially consultants).

This investigation focuses on the predictive modelling of drainage water quality from mine waste facilities by means of reactive transport modelling. The study presents a numerical model capable of simulating the key physicochemical processes occurring in the mine waste deposits by explicitly solving water flow, multicomponent solute transport, gas transport and geochemical reactions (Section 3). The latter is solved within the widely used geochemical code PHREEQC (e.g. Parkhurst & Appelo 2013), while the entire modelling framework is coded in MATLAB. This study also presents examples of predictive simulations at three particular mine sites in Finland illustrating the specific capabilities of the model formulation (Section 4). The data collected from the sites included mineralogical and chemical properties of the wastes and quality of drainage waters. The major weathering processes of the waste deposits were conceptualized by the dissolution of sulphide and other buffering minerals due to the penetration of recharge water as well as atmospheric oxygen into the waste dump systems. These simulation examples also generally demonstrate how reactive transport modelling can be used in the attempt of predicting the seepage water compositions from mine waste settings. Among the presented examples, the first two cases include the modelling within waste rock piles (Sections 4.2-4.3), whereas the third one represents the simulations in a tailings impoundment (Section 4.4). Based on the quantity of the available information at individual sites and the view point of the modelling exercises, these examples can be treated as the predictions in proposed “future” waste dumps although some of these waste facilities currently exist. Note that though the presented simulations were limited to the simplified assumptions of 1-D reactive transport scenarios, the model formulation is also flexible to adopt in multiple dimensions or to implement more complex flow conditions. For each modelling exercise, predictive analysis was also extended to evaluate the sensitivity of the key parameters as well as to predict long-term behaviour of waste piles under closure scenarios. The simulation results suggest that numerical modelling in combination with good quality data provides the potential to quantitatively interpret the timing and occurrence of future toxic drainages that maybe dangerous to the surrounding receptors. However, care must be taken when dealing with the specific outcomes of the modelling as they might be subjected to significant extent of uncertainty. The later part of this report includes a discussion about the major sources of uncertainties in the presented cases (Section 4.5), and general guidance on the modelling aspects one should be aware of when conducting predictive simulations (Section 5).

2 SITE DESCRIPTIONS AND DATA COLLECTION

Mine waste and drainage water samples were collected from three mine sites around Finland. The waste rock samples composed of 15–20 kg composite samples, with individual fist-sized subsamples collected from around 10 × 10 m area. Tailings samples composed of 5–10 kg composite samples collected from the surface and from the deeper less weathered part of the tailings. Drainage samples were collected from seepage points below the waste material sampling points.

2.1 Kylylahti

Kylylahti Cu-Co-Zn-Ni-Au mine is located in Polvijärvi municipality, North Karelia region in eastern Finland. The ore body was found in 1984, but the construction of the underground mine was commenced not until 2010 and the mine started to operate in the summer of 2012. Ore is being extracted at a rate of around 550,000 t/y and it has been estimated to be depleted in 2021. The ore from the Kylylahti is being processed at the Luikonlahti processing plant in Kaavi municipality around 43 km west from the mine site. Therefore, there are no tailings deposited in the Kylylahti area. The waste rock pile is temporary, as most of the waste rock material will be backfilled to the underground mining tunnels. (Kylylahti Copper Oy 2006, Boliden 2014)

The Kylylahti ore deposit is a mafic-ultramafic volcanogenic massive sulphide deposit (VMS), which is hosted by quartz rocks and metacarbonates (Kontinen et al. 2006, GTK 2018). The waste rocks are compose mainly of mica schists and serpentinites (Kylylahti Copper Oy 2006). The main sulphides are pyrite, pyrrhotite, chalcopyrite, and sphalerite (Kontinen et al. 2006).

2.2 Särkiniemi

Särkiniemi Ni mine is located in Leppävirta municipality, North Savonia region in eastern Finland. Although a larger mine, Kotalahti, was operating from 1959 to 1987 only three kilometers away, the Särkiniemi deposit was found only at the beginning of 1990's. Finn Nickel Oy started the exploitation of the deposit in 2007. Due to low nickel prices the activities were ceased and the company was declared bankruptcy in 2009 (Räisänen et al. 2017).

Bedrock of the area mainly consists of mica schists, peridotites and gabbro. The deposit is composed of two parts, of which the eastern is hosted by gabbros, and the western by peridotite. The main ore minerals in the deposit are pyrrhotite, pentlandite and chalcopyrite. Originally, the ore reserve was estimated to be 0.12 Mt, including 0.92% Ni and 0.44% Cu (Makkonen & Halkoaho 2007, Makkonen 2015)

Around 0.1 Mt of ore was excavated from the open pit and the underground mine. The ore was processed at the Hitura processing plant. Therefore, no tailings have been deposited at the Särkiniemi mine site. Around 38,000 t of waste rock was excavated, of which around 25,000 t was located into the open pit. Part of the waste rock was initially crushed for aggregates, but was eventually deposited at the mine site, since it was noticed that the material was strongly

acid producing and not suitable for utilisation. The rest of the waste rocks were deposited in the waste rock pile, which has been partly covered with till (Räisänen et al. 2017).

2.3 Pyhäsalmi

The Pyhäsalmi Cu-Zn mine is located in Pyhäjärvi municipality, Northern Ostrobothnia region. The mining activities were commenced in 1962 as open pit, which continued till 1975. In 1967, also underground mining was commenced. The mining activities have been estimated to cease in 2019, after which the mine will be closed. Since 1990, the annual production of underground mining has been over 1 Mt (Pohjois-Suomen AVI 2007).

The Pyhäsalmi deposit is massive, coarsely grained sulfide ore. The main minerals are pyrite, sphalerite, chalcopyrite and pyrrhotite, and in lesser amounts galena. The underground mine does not produce sufficiently waste rocks for the backfilling of the mine. Therefore additional rocks must be excavated from a separate quarry. Tailings have been deposited in a facility, which has been divided into four sections (A, B, C and D ponds), of which the A-pond has been decommissioned and closed between the years 2001 and 2002 (Pohjois-Suomen AVI 2007).

2.4 Analytical methods

Mine waste and drainage water samples were analysed in an accredited laboratory of Labtium Oy. Drainage water analyses included determination of dissolved element concentrations by ICP-OES and ICP-MS methods and determination of anions with ion chromatography. Electrical conductivity and pH of the drainage waters were measured at the site using a portable multi-parameter YSI sonde (YSI Professional Plus).

For geochemical analyses, the waste rock samples were dried below 40 °C, crushed with Mn-jaw crusher and ground in a hardened steel bowl. The tailings samples were freeze-dried and sieved to < 2 mm grain size for the partial extraction. The total element concentrations were determined by the XRF method (Criss & Birks 1968) and the fractions bound to sulphide phases by the Aqua Regia extraction (Doležal et al. 1968, Heikkinen & Räisänen 2009). All the sample solutions were measured by ICP-OES and ICP-MS. Potential of the mine wastes to produce ARD was determined by the ABA test according to the standard EN 15875 (CEN 2011) and by the NAG test (AMIRA 2002).

Mineralogical investigation of the mine waste samples was conducted at the mineralogical laboratory of Geological Survey of Finland (GTK). The analyses were performed by a field emission scanning electron microscope (FE-SEM; JEOL JSM 7100F Schottky) with automated energy dispersive spectrometer (EDS; Oxford Instruments EDS X-Max 80 mm^2). Identification of minerals was performed based on the comparison of the element composition by EDS spectra to the in-house mineralogical database of GTK.

3 MODELLING APPROACH

Based on the collected data at the three mine sites, predictive analysis was performed to quantify the drainage water quality from the waste deposits. Particularly, the prediction was performed with reactive transport modelling by taking into account the mineralogical compositions as well as recharge through the waste material. The fundamental steps of the modelling approach is briefly explained in this section.

3.1 Water Flow and Solute Transport Equations

In mine waste systems, acid generation processes typically occur in the unsaturated zones, where water flow in such variably saturated porous media is typically described by Richards equation. Under the assumption of negligible hysteresis, incompressible liquid, and a passive air phase, Richards equation can be written as (e.g. Neuman 1973):

$$S_s S_w \frac{\partial h}{\partial t} + \theta \frac{\partial S_w}{\partial t} - \nabla \cdot \left(k_r \mathbf{K} \nabla h \right) = Q_i^w \qquad (1)$$

where S_s [L^{-1}] is the specific storage coefficient, S_w [-] is the water saturation, h [L] defines hydraulic head, θ [-] is the porosity, t [T] is time, k_r [-] is relative permeability of aqueous phase, $\mathbf{K}$ [LT^{-1}] denotes the hydraulic conductivity tensor, and Q_i^w is the source/sink term [T^{-1}]. The relationship between the relative permeability and aqueous phase saturation is commonly described by the empirical formulations of soil hydraulics such as van Genuchten parameterisation (e.g. Wösten & van Genuchten 1988), among others.

The multicomponent transport of dissolved species within the aqueous phase coupled with chemical reactions is described by the governing equations of classical advection-dispersion transport and taking into account the reaction terms (e.g. Steefel and Lasaga 1994):

$$\frac{\partial}{\partial t}\left(\theta S_w C_i\right) = -\left(\mathbf{q} C_i\right) + \nabla \cdot \left(\theta S_w \mathbf{D}_i \nabla C_i\right) - \sum_{r=1}^{N_r} \upsilon_{ir} R_r - \sum_{m=1}^{N_m} \upsilon_{im} R_m - \sum_{r=1}^{N_g} \upsilon_{ig} R_g \qquad (2)$$

where C_i [ML^{-3} water] is the concentration of species i, $\mathbf{q}$ [LT^{-1}] is the vector for Darcy velocity, $\mathbf{D}_i$ [L^2T^{-1}] denotes the dispersion tensor for species i, and R_r, R_m, R_g [$ML^{-3}T^{-1}$] and υ_{ir}, υ_{im}, υ_{ig} [-] are the reaction rates and stoichiometric coefficients in aqueous phase, minerals and gas phase, respectively. Please note that for the multicomponent transport of ionic species, a more accurate representation of the diffusion/dispersion term in the above equation should be based on the Nernst-Planck equations explicitly taking into account the electrostatic interactions among charged solutes as well as charged surfaces (e.g. Ben-Yaakov 1972, Lasaga 1979, Boudreau et al. 2004, Appelo & Wersin 2007, Cussler 2009, Muniruzzaman et al. 2014). However, for the sake of simplicity this electrical potential term is ignored in this particular work and the modelling of all the solute species transport was treated as uncharged solutes. These simplifications are probably justifiable for the presented modelling scenarios as the site-specific

information does not allow constraining all these details to be embedded in the model. For dispersion parameterisation, the classical linear parameterisation (Scheidegger 1961) was used even though it is often criticised for having a too simplistic formulation and inability to capture small scale physical processes especially in heterogeneous formations:

$$D_i = D_{p,i} + \alpha\left(\frac{q}{\theta S_w}\right) \tag{3}$$

where $D_{p,i}$ [L^2T^{-1}] is the pore diffusion coefficient of solute i in the aqueous phase, α [L] is the dispersivity of the porous medium, and q [LT^{-1}] is the Darcy velocity component in a specific direction. D_p is typically approximated with the Archie's law (Archie 1942), among other functional relationships:

$$D_{p,i} = \left(\theta S_w\right)^n D_i^w \tag{4}$$

with D_i^w [L^2T^{-1}] and n [-] being the molecular diffusion coefficient in the aqueous phase and an empirical exponent, respectively.

3.2 Gas Transport Equations

Transport of gaseous phases is an important mechanism in sulphide weathering processes as it effectively provides the supply of the primary reactant (oxygen) into the system. Although in real systems the transport of gas into the waste facilities can be driven by convective air flow as well as diffusion, the presented cases in this study only consider the diffusive gas transport to formulate a relatively simple model. The simplest description of gas diffusion in a variably saturated domain can be expressed by Fick's law, which takes the form:

$$\frac{\partial}{\partial t}\left(\theta S_g C_i^g\right) = \nabla \cdot \left(\theta S_g \mathbf{D}_{p,i}^g \nabla C_i^g\right) - Q_i^g \tag{5}$$

where S_g [-] is the gas phase saturation, C_i^g is the gas phase concentration of species i [ML^{-3} gas], $\mathbf{D}_{p,i}^g$ [L^2T^{-1}] represents the tensor containing pore diffusion coefficient, and Q_i^g [$ML^{-3}T^{-1}$] is the source/sink term in the gas phase. The pore-diffusion coefficient, which is the free-phase diffusion in gas normalized by the tortuosity, in the above equation is typically estimated as a function of gas-filled porosity. In this work, the semi-empirical expression of Millington (1959) was used to calculate pore diffusion coefficients in the gas phase:

$$D_{p,i}^g = \theta^{1/3} S_g^{1/7} D_i^g \tag{6}$$

in which D_i^g [L^2T^{-1}] is the molecular diffusion coefficient of species i in gas phase.

3.3 Geochemical Reactions

3.3.1 Mineral dissolution/precipitation and aqueous phase reactions

Geochemical processes occurring in the mine wastes are simulated with the widely used USGS's geochemical code PHREEQC (Parkhurst & Appelo 2013). For each test site, important acid producing minerals and buffering minerals were identified by mineralogical analysis (Section 2) of the waste samples. Thermodynamic properties as well as kinetic rate laws of the relevant minerals were compiled in a customized database because none of the standard databases provide all the required minerals. Table 1 summarises the fundamental chemical reactions for dissolution/precipitation of all the minerals used in this study along with their corresponding equilibrium constants.

3.3.2 Kinetics of mineral dissolution/precipitation reactions and rate laws

The geochemical reactions governing the dissolution of primary minerals were considered kinetically controlled in the predictive modelling. The corresponding rate laws for different minerals used in the simulations are summarised in Table 2. For brevity, only the oxidation of sulphide minerals by oxygen was implemented in the simulations. However, additional reaction pathways including the oxidation by Fe(III) can also be easily implemented in the current formulation but such mechanisms seemed to be too fast compared to the measured drainage chemistry. In order to confirm such mechanisms, further information regarding the microbial activity is required at the specific test sites.

Please note that in Table 2 the first term in the rate expression ($A_{sp}m_0$) [m^2] of sulphide minerals represents the total surface area of the mineral: where A_{sp} [m^2mol^{-1}] is the specific surface area of the mineral (i.e. surface area per unit mass), m_0 [mol] is the initial amount of the mineral, and V_w [L] is the volume of pore water. The last term (1- *IAP/K*) ensures that the mineral dissolution/precipitation rate reduces to zero towards the equilibrium for reversible reactions. Also notice that the second term of the expression $((m/m_0)^{2/3})$ represents the evolution of the reactive mineral surface area as the particle size decreases with the progress of reaction and destruction of weathering mineral particles. Consequently, it leads to the decrease of the overall reactivity over time during the mineral dissolution processes because the surface area of the mineral is directly proportional to the ratio between unreacted and initial mineral amount (m/m_0). This approach allows adopting the element of the shrinking core model (e.g. Levenspiel 1972, Wunderly 1996) by implicitly mimicking the limitations of oxidation rates through the reacted surface layer. However, the rate expression, explicitly considering the evolution of surface area as well as core radius, can also be easily implemented in the current framework but realistic transport coefficients through the so called "ash layer" (e.g. Wunderly et al. 1996) in such formulation is often difficult to obtain.

A similar approach was also used in the rate expressions for the reactions of carbonate minerals (Table 2). However, this rate law was adopted from Plummer et al. (1978), which suggests three different dissolution/precipitation pathways representing acidic, neutral, and carbonate mechanisms, respectively, for dolomite and calcite dissolutions.

Table 1: Mineral dissolution/precipitation reactions used in the reactive transport simulations

Mineral	Reaction	log *K*
Pyrite	$FeS_2 + 2H^+ + 2e^- \rightarrow Fe^{2+} + 2HS^-$	-18.479[a]
Pyrrhotite	$Fe_{0.87}S + H^+ + 0.26e^- \rightarrow 0.87Fe^{2+} + HS^-$	-5.59[b]
Pentlandite	$Fe_{4.5}Ni_{4.5}S_8 + 16.5O_2 + 2H^+ \rightarrow 4.5Fe^{2+} + 4.5Ni^{2+} + 8SO_4^{2-} + H_2O$	-[c]
Sphalerite	$ZnS + H^+ \rightarrow Zn^{2+} + HS^-$	-11.618[d]
Chalcopyrite	$CuFeS_2 + 2H^+ \rightarrow Cu^{2+} + Fe^{2+} + 2HS^-$	-35.27[d]
Aqueous speciation reactions coupled to sulphide mineral reactions		
	$2H_2O \rightarrow O_2 + 4H^+ + 4e^-$	-86.08[a]
	$SO_4^{2-} + 9H^+ + 8e^- \rightarrow HS^- + 4H_2O$	33.65[a]
Calcite	$CaCO_3 \rightarrow Ca^{2+} + CO_3^{2-}$	-8.48[a]
Dolomite	$CaMg(CO_3)_2 \rightarrow Ca^{2+} + Mg^{2+} + 2CO_3^{2-}$	-17.09[a]
Biotite	$KMg_3AlSi_3O_{10}(OH)_2 + 10H^+ \rightarrow K^+ + Al^{3+} + 3Mg^{2+} + 3H_4SiO_4$	43.30[d]
Chlorite	$Mg_5Al_2Si_3O_{10}(OH)_8 + 14H^+ \rightarrow 5Mg^{2+} + 2Al^{3+} + 3Mg^{2+} + 3H_4SiO_4 + 6H_2O$	68.38[d]
Tremolite	$Ca_2Mg_5Si_8O_{22}(OH)_2 + 14H^+ + H_2O \rightarrow 2Ca^{2+} + 5Mg^{2+} + 8H_4SiO_4$	56.574[d]
Hornblende	$Ca_2Mg_{2.8}Fe_{2.2}Si_8O_{22}(OH)_2 + 14H^+ \rightarrow 2Ca^{2+} + 2.8Mg^{2+} + 2.2Fe^{2+} + 8SiO_2 + 8H_2O$	61.24[e]
Serpentine	$Mg_{2.77}Fe_{0.23}Si_2O_5(OH)_4 + 6H^+ \rightarrow 2.77Mg^{2+} + 0.23Fe^{2+} + 2SiO_2 + 5H_2O$	500.16[e]
Anthophyllite	$Mg_7Si_8O_{22}(OH)_2 + 14H^+ \rightarrow 7Mg^{2+} + 0.23Fe^{2+} + 8SiO_2 + 8H_2O$	66.80[e]
Albite	$NaAlSi_3O_8 + 8H_2O \rightarrow Na^+ + Al(OH)_4^- + 3H_4SiO_4$	-18.002[a]
K-Feldspar	$KAlSi_3O_8 + 8H_2O \rightarrow K^+ + Al(OH)_4^- + 3H_4SiO_4$	-20.573[a]
Siderite	$FeCO_3 \rightarrow Fe^{2+} + CO_3^{2-}$	-10.89[a]
Gibbsite	$Al(OH)_3 + 3H^+ \rightarrow Al^{3+} + 3H_2O$	8.11[a]
Ferrihydrite	$Fe(OH)_3 + 3H^+ \rightarrow Fe^{3+} + 3H_2O$	-4.891[a]
Goethite	$FeOOH + 3H^+ \rightarrow Fe^{3+} + 2H_2O$	-1.0 [a]
Jarosite-K	$KFe_3(SO_4)_2(OH)_6 + 6H^+ \rightarrow 3Fe^{3+} + 6H_2O + K^+ + 2SO_4^{2-}$	-9.21 [a]
Gypsum	$CaSO_4 \cdot 2H_2O \rightarrow Ca^{2+} + SO_4^{2-} + 2H_2O$	-4.58 [a]
Silica(a)	$SiO_2 + 2H_2O \rightarrow H_4SiO_4$	-2.71 [a]

[a] PHREEQC database
[b] SIT database
[c] Irreversible reaction, reaction stoichiometry after Jambor & Owens (1995) as adopted in Mayer et al. (2002)
[d] WATEQ4F database
[e] CrunchFlow database (lis-cis.dbs)
[f] LLNL database

For silicate minerals, the reactions were considered to be pH dependent and only the pathways at low pH conditions were implemented in the simulations. The specific surface area (A_{sp}) and the reaction rate constants (k) were mostly taken from the literature values obtained in the laboratory studies under controlled conditions.

Table 2: Rate expressions for mineral dissolution/precipitation reactions used in the simulations, r has units of [mol L^{-1} s^{-1}]

Mineral	Rate Law
Pyrite[1] Pyrrhotite[1] Chalcopyrite[1] Sphalerite[1]	$r = \frac{A_{sp} m_0}{V_w}\left(\frac{m}{m_0}\right)^{2/3}\left[k(O_2)^{0.50}(H^+)^{-0.11}\right]\left(1-\frac{IAP}{K}\right)$
Pentlandite[1]	$r = \frac{A_{sp} m_0}{V_w}\left(\frac{m}{m_0}\right)^{2/3}\left[k(O_2)^{0.50}(H^+)^{-0.11}\right]$
Calcite[2] Dolomite[2]	$r = \frac{A}{V_w}\left(\frac{m}{m_0}\right)^{2/3}\left[k_1(H^+)+k_2(H_2CO_3)+k_3(H_2O)\right]\left(1-\frac{IAP}{K}\right)$
Biotite[3]	$r = \frac{A}{V_w}k(H^+)^{0.25}$
Chlorite[4]	$r = \frac{A}{V_w}k(H^+)^{0.5}$
Tremolite[4]	$r = \frac{A}{V_w}\left[k_1(H^+)^{0.7}+k_2\right]$
Hornblende[4]	$r = \frac{A}{V_w}k(H^+)^{0.6}$
Serpentine[4]	$r = \frac{A}{V_w}k(H^+)^{0.31}$
Anthophyllite[4]	$r = \frac{A}{V_w}k(H^+)^{0.44}$
Albite[4]	$r = \frac{A}{V_w}k(H^+)^{0.46}$

[1] Rate law from Williamson & Rimstidt (1994), and adopted for shrinking core model by taking into account the reduction of mineral surface area as the reaction proceeds (Appelo & Postma 2005)

[2] Rate law from Plummer et al. (1978), and adopted for shrinking core model by taking into account the reduction of mineral surface area as the reaction proceeds (Appelo & Postma 2005)

[3] Nagy et al. (1995)

[4] Palandri & Kharaka (2004)

3.4 Numerical Solution

The governing equations describing the flow and transport as well as geochemical reactions in water and gas phases (Eqs. 1–6) were numerically solved in order to provide a quantitative description of the acid-mine drainage processes in mine waste deposits. Figure 1 illustrates a schematic diagram demonstrating the modelling approaches used in this study. An operator splitting scheme, employing the traditional sequential non-iterative approach (SNIA), was used to solve the reactive transport problem by decoupling the transport and reaction calculations. For the sake of simplicity and due to the lack of detailed site-specific information on soil hydraulics, or water saturation profiles the water flow problem through the waste facilities was not explicitly solved for the particular modelling exercises presented in this report. Instead, a uniform flow condition characterised by the annual average of the recharge rate at the corresponding study area was applied to describe the water flux through the simulation domain. The multicomponent transport problem of the dissolved constituents, both in the aqueous phase (Eq. 2) and gas phase (Eq. 5), was solved with the cell-centered finite volume method (FVM). An upwind differentiation scheme was used for the spatial discretisation of the transport equations with maintaining the Courant–Friedrichs–Lewy (CFL) stability criteria (i.e. $Cr \leq 1$). For the integration in time the explicit Euler method was used in the computation of advective fluxes, whereas the diffusion/dispersion problem in aqueous/gas phase was solved by using the implicit Euler time integration method. The resulting system of equations describing the aqueous and gas phase transport was solved with the direct matrix solver UMFPACK (Davis and Duff 1997). The calculation sequence is initiated by the simultaneous solution of aqueous and gas phase transport. Afterwards, the transported concentrations at each location of the discretised domain are updated and passed to reaction step for the calculations of gas-water partitioning and chemical reactions. The solubility of gases in the liquid phase was calculated within PHREEQC, which uses either Henry's law or Peng-Robinson EOS for ideal and non-ideal gases respectively (Parkhurst & Appelo 2013). The entire formulation of the presented modelling approach is implemented in MATLAB®.

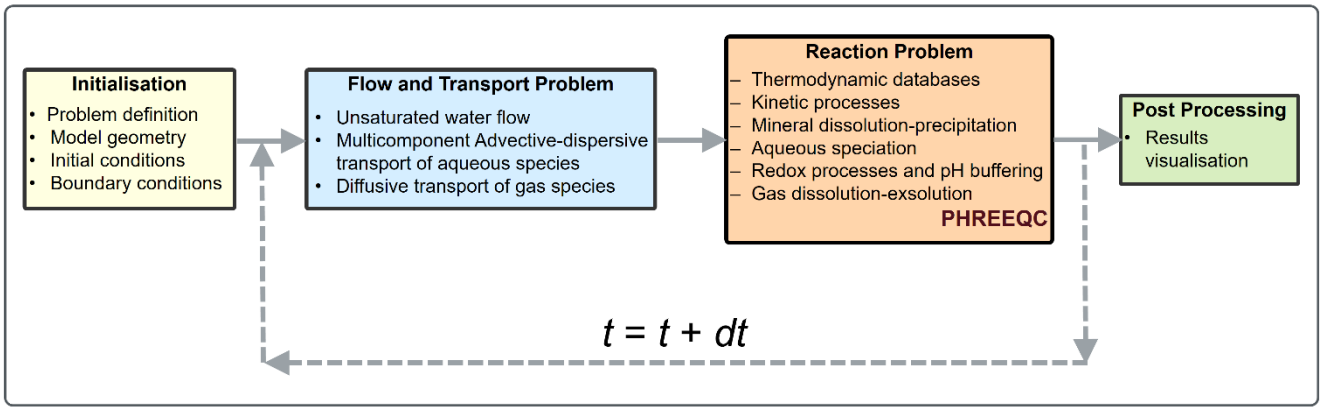

Figure 1: Schematic diagram of the structure and calculation steps of the modelling approach.

The geochemical reactions occurring in the mine waste systems were solved with the widely used open source geochemical code, PHREEQC from the United States Geological Survey. In particular, the reaction calculations were performed utilising the IPhreeqc module (Charlton & Parkhurst 2011), which is a specially designed module that enables using PHREEQC and its reaction capabilities in other programming/scripting languages and software programs. Coupling of this IPhreeqc module with other programs is particularly effective and involves particular advantage over traditional loosely coupled codes as it provides the opportunity to communicate between codes without writing or reading any external files (Charlton & Parkhurst 2011). The detailed approaches regarding the use of IPhreeqc and its coupling procedure is explained elsewhere (e.g. Wissmeier & Barry 2011, Müller et al. 2011, Nardi et al. 2014, Nasir et al. 2014, He et al. 2015, Korrani et al. 2015, Muniruzzaman et al. 2016). After solving the flow and transport problem, the matrices of concentrations and/or partial pressures of dissolved species in the aqueous and gas phase are sequentially passed to PHREEQC in order to perform geochemical reaction calculations (e.g. mineral dissolution/precipitation, aqueous speciation, and redox reactions). Particularly, in a time step (*dt*), the concentrations of all the dissolved constituents in the pore water as well the composition of O_2 and CO_2 after a transport step is updated to simulate geochemical processes. Such update is performed by utilising the PHREEQC keyword MODIFY, which allows modifying specific properties of a previously defined block (Parkhurst & Appelo 2013). The chemical reactions are computed by conceptualising as a batch reactor in each discretised grid block (control volume), containing reacting minerals and/or other physicochemical properties of interest, of the simulation domain. After the solution of chemical reactions within PHREEQC, the newly obtained pore water and gas phase compositions are transferred back to the transport model. The same sequence of these transport and reaction calculations continues in the next time steps. The formulation offers a relatively simple and yet rigorous platform taking into account the important processes controlling the reactive transport processes in mine wastes. Please note that in addition to the approach presented in the current formulation, these processes can also be solved with other reactive transport codes such as MIN3P (Mayer et al. 2002), HP1/HP2 (Simunek et al. 2012), CrunchFlow (Steefel & Lasaga 1994), TOUGHREACT (Xu & Pruess 2001), among others.

3.5 Benchmarking of the modelling approach

Before turning to more complex predictive simulations for specific mine sites, the presented modelling approach is benchmarked by comparing the modelling outcomes with PHREEQC for a 1-D reactive transport problem involving the oxidation of sulphide minerals and subsequent transport of released pore water species. Particularly, a simple 1-D scenario involving the solute transport and oxidation of sulphide minerals was solved with PHREEQC alone as well as with the presented coupled code incorporating IPhreeqc. This exercise considers only the dissolution of sulphides and biotite, which was assumed to have a consistent mineralogical composition as observed in the Särkiniemi waste rock materials (Table 3). The simulation domain was considered to be 3 m long, which was discretised into 50 cells. A constant water flux of 300 mm/y and a constant oxygen concentration resembling the atmospheric condition was applied at the inlet boundary of the domain. The kinetic rate laws,

the associated reaction parameters, and the relevant transport parameters are used as in Table 3. Since PHREEQC does not allow the calculation of gas transport, the simulations were performed by assuming a hypothetical condition of having an unlimited supply of oxygen phase throughout the domain. This example allows verification of the performance of the IPhreeqc coupling as well as the subsequent reactive transport calculations used in the current modelling approach.

Table 3: Initial mineral contents, reactive surface areas of minerals, and reaction rate coefficients.

Mineral	**Mineral Content**		**Surface Area, *A***	**Rate coefficient, *k***	**Reference**
	[wt%]	**[mol L_w^{-1}]**[a]	**[m^2 L_w^{-1}]**	**[mol m^{-2} s^{-1}]**	
Biotite	33.56	2.12	4	$10^{-10.97}$	Nagy (1995)
Pyrrhotite	1.52	0.50	81 [b]	$10^{-8.19}$	Williamson & Rimdstidt (1994)
Pentlandite	0.03	1.03×10^{-3}	100 [b]	$10^{-8.19}$	Williamson & Rimdstidt (1994)
Pyrite	0.02	4.42×10^{-3}	120[b]	$10^{-8.19}$	Williamson & Rimdstidt (1994)
$Fe(OH)_3(a)$[c]	-	-	-	-	PHREEQC Database

[a] Moles of mineral per liters of pore water, calculated from the wt% by using a solid density, ρ_s = 2.65 [kg L^{-1}] and an average porosity, θ = 0.50

[b] Surface area per moles of minerals per liters of pore water [$m^2mol^{-1}L_w^{-1}$]

[c] Simulated as equilibrium precipitation

Figure 2 represents the simulated spatial concentration profiles of the different elements and minerals after 10 years. Notice that, due to the absence of any effective buffering minerals (e.g. carbonates), pH of the effluent drops very quickly. This pH front is directly correlated to the increase of dissolved concentrations of different ions such as SO_4, Fe, and Ni. The agreement between the two simulation results, using PHREEQC alone (markers) and using the current modelling approach combined with IPhreeqc (lines), seems to be very good. Such outcomes validate the involving reactive transport calculations and the predictive modelling approach used in this study.

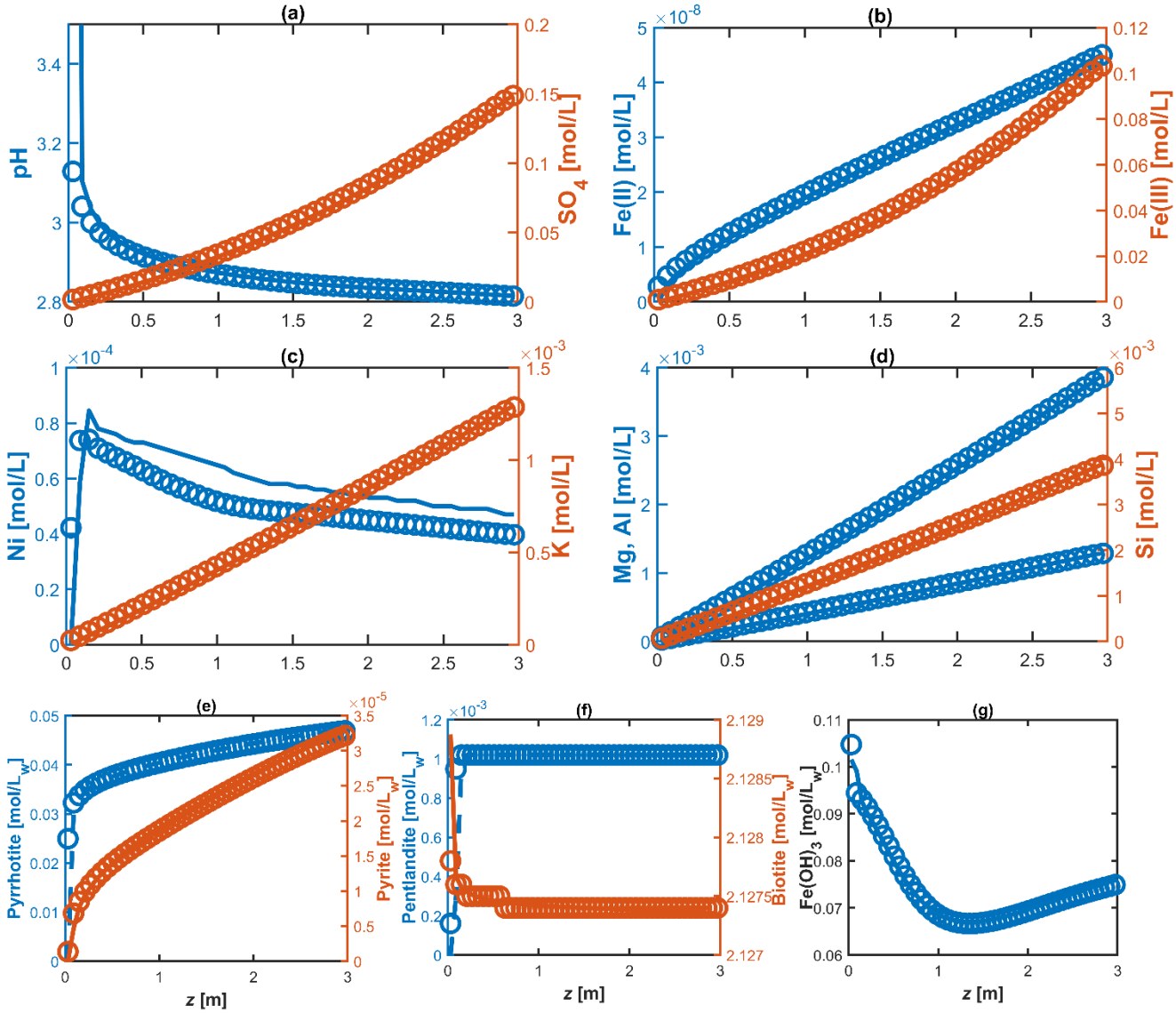

Figure 2: Profiles of the dissolved concentrations (a-d) and mineral contents (e-g) along the depth of the simulation domain. Lines represent the simulated concentrations using the coupled formulation as presented in this study, and the markers represent the simulation results from PHREEQC.

4 RESULTS AND DISCUSSION

Reactive transport modelling was performed in order to facilitate the long-term predictive analyses for waste drainage quality at different mine sites. Such analysis was based on the site-specific measurements such as mineralogy of the waste materials, compositions of the drainage water, and results from static tests. In this section, the results of the predictive simulations are summarised for three specific sites, in which the first two cases focus on the prediction of the drainage quality in waste rock dumps, and the last exercise corresponds to the predictive modelling in a tailings impoundment.

4.1 Conceptual model

The reactive transport simulations at different sites were performed based on the conceptual model as schematically illustrated in Figure 3. In particular, the predictive simulations considered a 1-D vertical simulation domain with homogeneous distributions of hydraulic properties and mineral assemblages. The mineralogical compositions were obtained from the measurements of waste deposits at each corresponding site. The size of the domain was used according to the specific waste settings in a specific mine site. At the top boundary of the domain, a constant influx of water was employed. The recharge water was considered to be in equilibrium with the atmosphere.

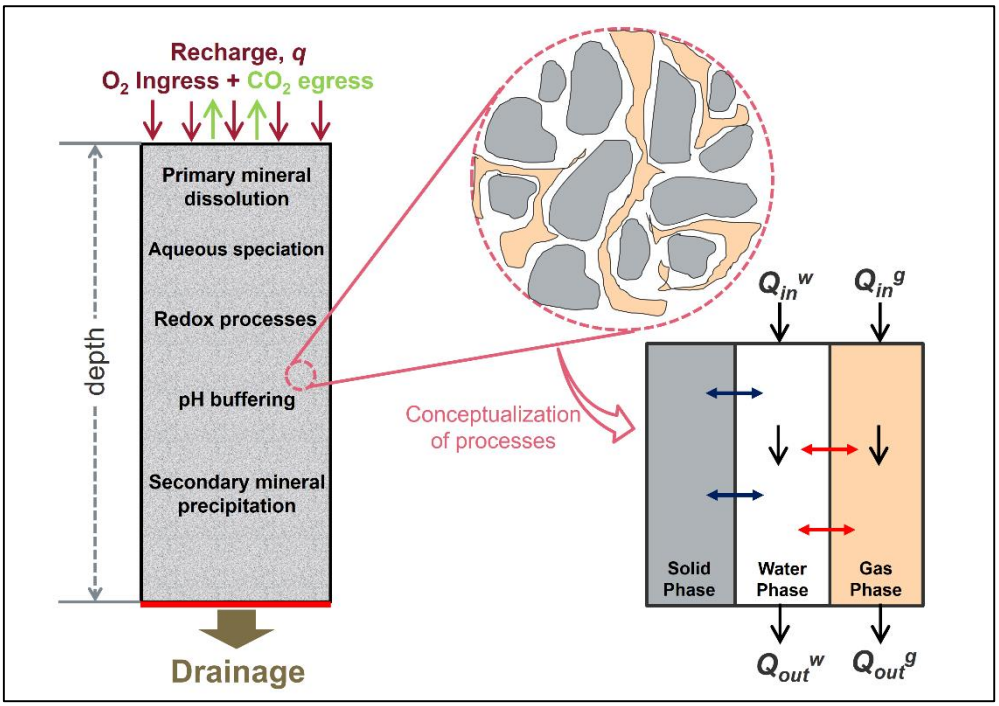

Figure 3: Conceptual model used in the predictive simulations in the waste piles and the general conceptualisation approaches of physicochemical system at different compartments of porous media.

The system was conceptualised as a three phase porous media with water, air, and solid matrix being the main phases (Figure 3). The model considers the transport in the aqueous and gas phases, while the solid phase is immobile. Inter-phase mass transfers were simulated in addition to the transport processes and geochemical reactions. The mineral dissolution-precipitation reactions were calculated following the procedures as outlined in section 3.

4.2 Modelling at Särkiniemi Waste Rock Pile

4.2.1 Problem definition and model input

The modelling for the Särkinemi site was performed along a vertical 1-D unsaturated domain resembling the reactive transport through the waste rock pile. Particularly, a domain of 10 m height was considered, which is consistent with the dimensions of the Särkiniemi waste rock pile. A constant recharge rate of 300 mm/y, which is ~50% of the mean annual precipitation in that region, was applied at the top boundary of the domain. However, there was no available information regarding the hydraulic properties such as porosity, permeability, moisture content, water/gas saturation curves and soil retention parameters and their spatial distributions in the waste rock pile. Therefore, a uniform seepage velocity of water identical to the recharge rate was assumed in the simulations. As the initial condition, the system was assumed to be in equilibrium with pure water, whereas a generic rainwater composition (Reimann et al. 1997) was used in the recharge water as the boundary condition. The recharge water was also assumed to be in equilibrium with atmospheric O_2 and CO_2. Table 4 summarises the hydraulic and transport parameters used in the simulation.

Table 4. Summary of geometry, flow and transport parameters used in the simulations.

Parameters	Values
Domain size (L_z) [m]	10
Discretisation, Δz [cm]	6
Time step, Δt [s]	3153600
Recharge rate, q [mm y^{-1}]	300
Solid density, ρ_s [kg L^{-1}]	2.65
Average porosity, θ [-]	0.50
Diffusion coefficient in aqueous phase, D^w [m^2s^{-1}]	2.00×10^{-9}
Longitudinal dispersivity, α_L [m]	10^{-3}
Diffusion coefficient in gas phase, D^g [m^2s^{-1}]	1.75×10^{-5}
Partial pressures of gas phase at the top boundary	
pO_2 [atm]	$10^{-0.67}$
pCO_2 [atm]	$10^{-3.50}$

The mineralogy of the waste rock materials at Särkiniemi Ni-mine site involves biotite, plagioclase, quartz, hornblende, and sulphides. The waste rock was identified as potentially acid producing by performing static tests with the waste materials (with NPR = 0.2-0.4 and

NAG pH = 2.7-2.9) (cf. Karlsson et al. 2018). The mineralogical assemblage suggests that sulphide content is approximately 2.85 – 3.32 wt%, in which pyrrhotite is the major sulphide-bearing mineral with smaller fractions of pyrite, pentlandite and chalcopyrite. The material does not contain any carbonates and the pH buffering mainly relies on the silicate minerals. The simulations were performed by considering pyrrhotite, pyrite, pentlandite, biotite, hornblende, serpentine, chlorite and anthophyllite as primary minerals. Table 5 summarises the contents of these minerals used in simulations. The model also considered ferrihydrite, gypsum, jarosite, gibbsite, and amorphous silica as secondary minerals. The dissolution of all the primary minerals were considered kinetically controlled, whereas equilibrium dissolution/precipitation was assumed for all the secondary mineral phases except silica for simplicity.

Table 5: Initial mineral contents, reactive surface areas of minerals, and reaction rate coefficients.

Mineral	Mineral Content		Surface Area, *A*	Rate coefficient, *k*	Reference
	[wt%]	[mol L_w^{-1}][a]	[m^2 L_w^{-1}]	[mol m^{-2} s^{-1}]	
Biotite	33.56	2.12	0.65	$10^{-10.97}$	Nagy (1995)
Hornblende	6.07	0.58	0.05	$10^{-8.10}$	Palandri & Kharaka (2004)
Serpentine	3.52	0.33	0.05	$10^{-9.08}$	Declercq & Oelkers (2014)
Albite	1.45	0.15	0.60	$10^{-10.16}$	Palandri & Kharaka (2004)
Chlorite	1.35	0.06	0.50	$10^{-11.11}$	Palandri & Kharaka (2004)
Pyrrhotite	1.52	0.50	0.30 [b]	$10^{-8.19}$	Williamson & Rimdstidt (1994)
Anthophyllite	0.45	1.53×10^{-2}	0.50	$10^{-11.94}$	Palandri & Kharaka (2004)
Pentlandite	0.03	1.03×10^{-3}	0.70 [b]	$10^{-8.19}$	Williamson & Rimdstidt (1994)
Pyrite	0.02	4.42×10^{-3}	0.30[b]	$10^{-8.19}$	Williamson & Rimdstidt (1994)
SiO_2(a)[c]	-	-	-	$10^{-10.5}$	Rimstidt & Barnes (1980)

[a] Moles of mineral per liters of pore water, calculated from the wt% by using a solid density, ρ_s = 2.65 [kg L^{-1}] and an average porosity, θ = 0.50

[b] Surface area per moles of minerals per liters of pore water [$m^2mol^{-1}L_w^{-1}$]

[b] Both kinetic parameters and equilibrium constant was slightly adjusted to be in the consistent drainage concentration range as the measured values

The oxidation of sulphide minerals were driven by the transport of water as well as diffusion of oxygen into the waste rock pile. The oxidation processes of sulphide minerals were modelled within PHREEQC with implementing the widely used rate law of Williamson & Rimstidt (1994) and by adopting the dependency of the reaction rate to mineral surface area as outlined in section 3.3. The kinetics of the silicate minerals were considered to be proportional to pH and only the acidic dissolution mechanisms were considered in the model. The sulphide minerals

were modelled as reversible reactions reacted to equilibrium conditions, whereas the silicate minerals were modelled as irreversible reactions. The values of the rate coefficients as well as reactive surface areas for different minerals used in the simulations of this particular exercise are summarised in Table 5. All the rate constants and the corresponding reaction orders are taken from the literature, whereas the reactive surface areas are slightly adjusted to yield a consistent drainage concentration with the measured values (Table 5).

4.2.2 Evolution of the drainage chemistry and minerals

Figure 4 shows the evolution of the drainage chemistry over time at the outlet of the waste rock pile. The trends of the simulated aqueous concentrations seem to follow a pattern dominated by the sulphide mineral oxidation processes. The pH values drop rather fast in the drainage water due to the oxidation of pyrrhotite, pyrite, and pentlandite and because of the absence of any carbonate mineral to effectively buffer the pH (Figure 4a). This oxidation processes also lead to elevated concentrations of the dissolved ions: SO_4, Mg, Fe, Ni, Al, Si, Ca, K, Na (Figure 4a-c). In this model, the Al and Si are mainly released from the dissolution of aluminosilicate minerals, which is facilitated by the low pH condition. Additionally, the increase in major ions (Ca, Mg, Na, and K) was also considered to be primarily coming from the silicate minerals in this particular calculation, whereas additional mechanisms might also be involved in reality. However, the front of the increase in these dissolved species' concentrations seem to be directly correlated to the drop in pH front (Figure 4a) as well the increase in electrical conductivity values (Figure 4d). Please note that the simulated concentrations also seem to be consistent with the measured values in the drainage water (Table 6) represented by the dotted lines with the corresponding colour for each species in Figure 4.

This drainage concentration measurement was performed approximately after 8 years of the construction of the waste rock pile. Although a few of these species (e.g. Fe, Na) show slight discrepancy between the simulated and measured concentrations, the values are evidently in the similar order for all the dissolved species. Interestingly, the total dissolved constituents also agree fairly well between the simulated and measured values as indicated in the electrical conductivity curve (Figure 4d). This is quite noteworthy given the fact that the results are from a rather simplistic model compared to the real waste rock pile system. The simulated value of pH at the late time plateau in Figure 4a is also consistent with the NAG pH (2.7-2.9) value obtained from the NAG test performed with the waste rock samples (section 2).

Table 6: Chemical composition of the recharge and drainage water for Särkiniemi waste rock pile

Species	Recharge Water		Drainage Water	
	[µg L^{-1}]	[mol L^{-1}][a]	[µg L^{-1}]	[mol L^{-1}]
Al	2.9	3.32×10^{-9}	10600	3.93×10^{-4}
S	290	9.04×10^{-6}	219000	6.83×10^{-3}
Fe	<1.00	7.46×10^{-10}	6230	1.12×10^{-4}
Mn	2.10	1.64×10^{-9}	2890	5.26×10^{-5}
As	0.08	7.42×10^{-11}	1.56	2.08×10^{-8}
Cd	0.06	3.71×10^{-11}	1.15	1.02×10^{-8}
Co	<0.002	3.39×10^{-11}	576	9.77×10^{-8}
Cr	<0.20	2.67×10^{-10}	0.86	1.65×10^{-8}
Cu	0.51	5.57×10^{-10}	231	3.63×10^{-8}
Mo	<0.03	2.17×10^{-11}	<0.02	2.08×10^{-10}
Ni	0.09	1.06×10^{-10}	6830	1.16×10^{-4}
Pb	0.56	1.88×10^{-10}	0.54	2.61×10^{-9}
V	0.07	9.54×10^{-11}	0.06	1.18×10^{-9}
Ca	50	1.25×10^{-6}	46700	1.17×10^{-3}
K	5.00	5.33×10^{-9}	5680	1.45×10^{-4}
Mg	2.00	3.43×10^{-9}	80700	3.32×10^{-3}
Na	<100	4.35×10^{-6}	3170	1.38×10^{-4}
Zn	5.7	3.26×10^{-9}	410	6.27×10^{-6}
Si	<100	3.56×10^{-6}	14700	5.23×10^{-4}
SO_4	500	5.21×10^{-6}	610000	6.35×10^{-3}
pH	4.9		3.3	
EC	8		1232[a]	

[a] Reimann et al. (1997)
[b] has a unit of [µS/cm]

Figure 5 illustrates the vertical penetration of gas phases into the waste rock pile. The transport of gas phases were simulated by gas diffusion only. It is evident from the figure that the diffusion of O_2(g) and CO_2(g) phases is significantly fast in the unsaturated simulation domain, which is typical for waste rock piles. Due to a smaller water saturation, O_2(g) is able to propagate deeper in the domain within a few years, and after only 3-4 years oxygen phase seem to saturate the domain (Figure 4a). Such assumptions, as used in this simulation, are not unrealistic for the waste rock piles as they are mainly unsaturated with respective to the water phase, and the effective ingress of air from the outside environment is somewhat common. Furthermore, in real multidimensional systems, in addition to the diffusive transport, convective air flow (both in the longitudinal and transverse directions) also ensures the supply of gas phases. These gas transport mechanisms are presumably orders of magnitude faster than the water phase transport and often the sulphide oxidation reactions. Consequently, these type of systems can be assumed and modelled as “semi-open” systems (e.g. Mayer et al. 2015). Therefore, it is only reasonable to treat the O_2(g) transport in unsaturated systems in a way that assures the abundance of gas supply compared to the other reactants or reaction kinetics.

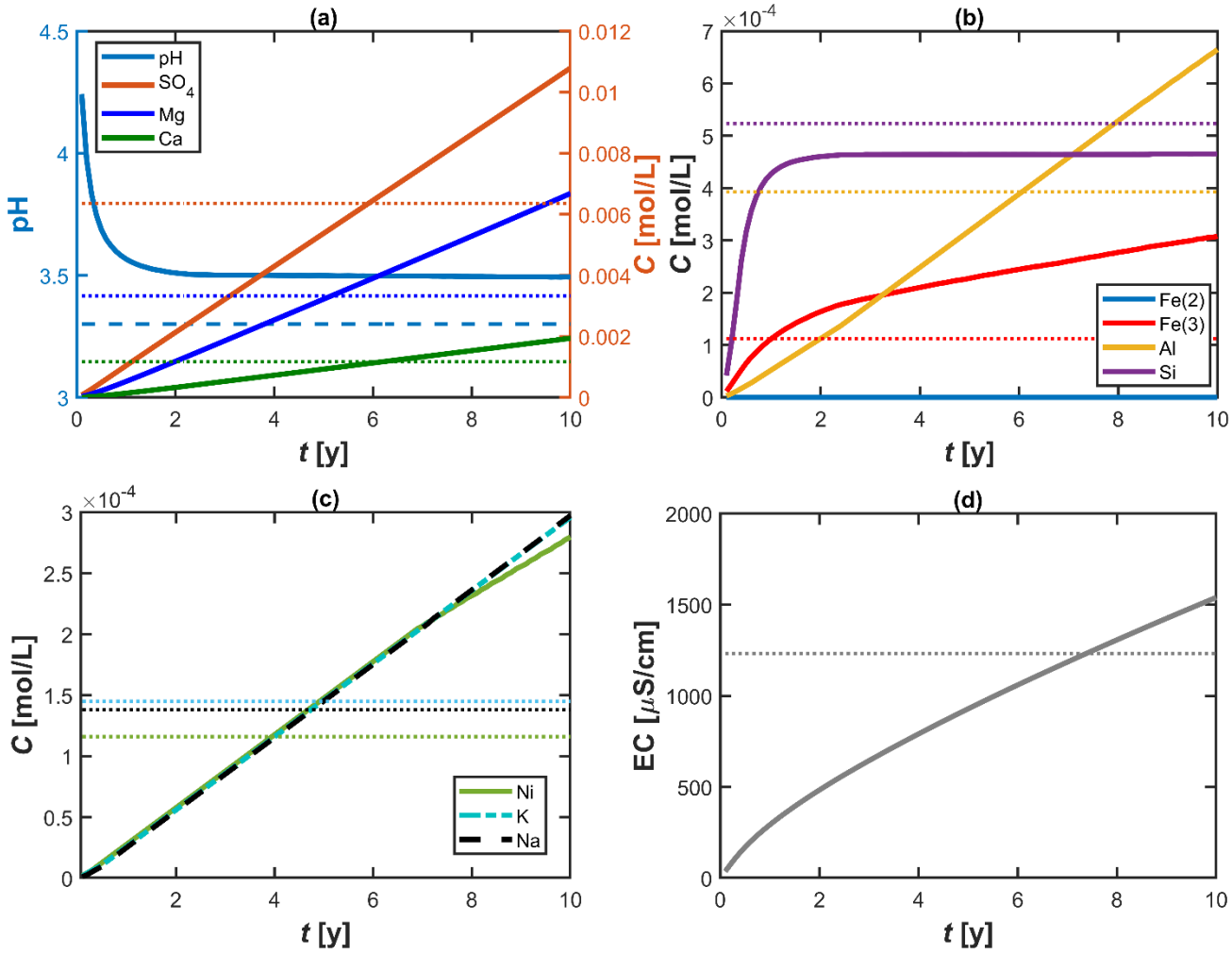

Figure 4: Simulated (solid lines) and measured (dotted lines) compositions of the drainage water from the Särkiniemi waste rock pile as a function of time: (a) pH (primary *y*-axis), SO_4, Mg, Ca (secondary *y*-axis), (b) Fe, Al, Si, (c) Na, K, Ni, and (d) electrical conductivity of drainage water.

However, notice that even though the propagation of gas phases seem to be significantly fast, the overall progress of the reactive processes, i.e. the oxidation of sulphides and the subsequent dissolution of aluminosilicates, is still limited by the solubility of oxygen in the aqueous phase. Such solubility, modelled by Henry's law or Peng-Robinson equation of states, is typically low and it makes the overall depletion of the reacting mineral phases a rather long process. Such phenomena is also indicated in Figure 6, which shows a fairly small net depletion of the different minerals compared to their initial mineral contents at the end of 10 years. Since the mineralogy of this particular case does not involve any carbonate mineral, there is no noticeable production of CO_2(g) in the system.

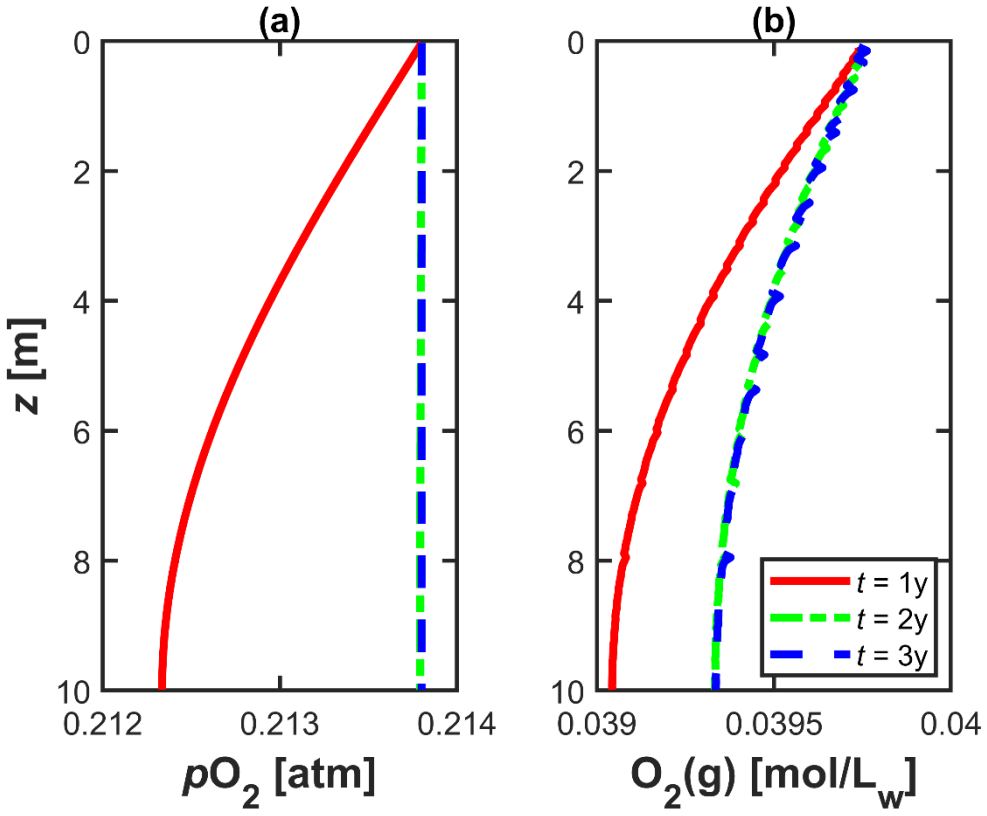

Figure 5: Evolution of O_2 partial pressures (a) and gas phase compositions (i.e. moles of oxygen in gas phase per L of pore water) (b) over depth of the Särkiniemi waste rock pile at different times.

Figure 6 shows the computed mineral fractions over depths at different simulation times. As the time progress, the primary minerals successively become depleted whereas the precipitation of a few secondary minerals are observed. As expected, a signature of the enhanced depletion of different minerals is clearly observed at the shallow depths where the oxygen influx is the steepest. In this simulation ferrihydrite, gypsum and amorphous silica were allowed to precipitate as secondary minerals.

It is evident from this figure that the elevated concentrations in the drainage water, as demonstrated in Figure 4, result from the dissolution of the primary minerals. For instance, the front associated with pH, SO_4, Fe, and Ni concentrations is directly connected to the dissolution fronts of pyrrhotite, pyrite, and pentlandite (Figure 4a-b and 6a-c). The concentrations of protons and Fe are also limited by the precipitation of the ferrihydrite phase (Figure 4a-b and 7a). The rise in the concentration of other ions (Al, Si, Ca, Mg, Na, and K) is mainly correlated to the dissolution fronts of the aluminosilicate minerals (Figure 6d-i). Such dissolution processes are accelerated in the low pH conditions.

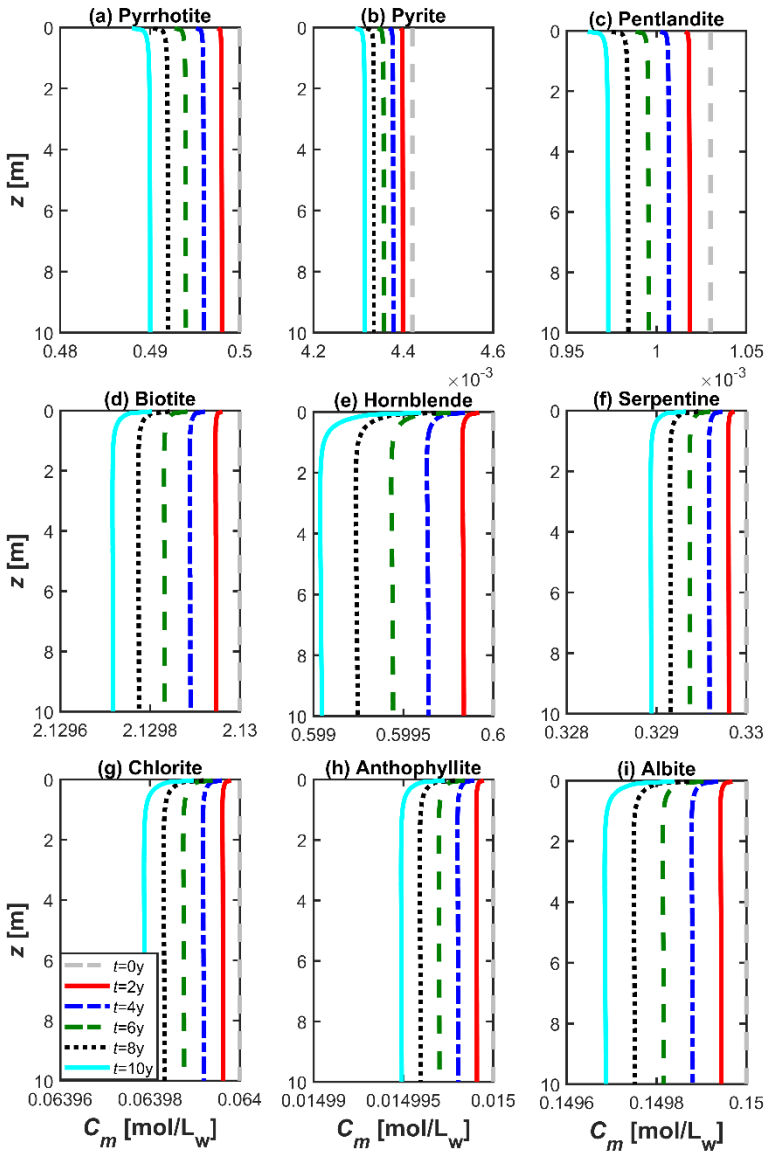

Figure 6: Evolution of mineral contents versus depth for the primary minerals in Särkiniemi waste rock pile.

Dissolved sulphate and calcium concentrations are controlled by the equilibrium with gypsum. However, the precipitation of gypsum was not observed in this particular case during the simulation duration (10 years) (Figure 7c). Therefore, sulphate concentration can be directly used as a proxy for the extent of sulphide dissolution reactions. Si concentration is also controlled by the secondary precipitation of silica phases as demonstrated in Figure 7. However, the equilibrium precipitation of SiO_2(a) was still producing a significant

overestimation of Si concentration compared to the measured value in the drainage water (Table 6). Hence, a kinetic precipitation of the silica phase was employed in the model with a slight adjustment of the rate coefficients as well as the equilibrium constants. In fact, only with this procedure and adjustments for the silica phase was it possible to simulate Si and other major ions (Al, Ca, Mg, Na, and K) in the drainage water in a way that is consistent with the measurement (Table 6, Figure 4).

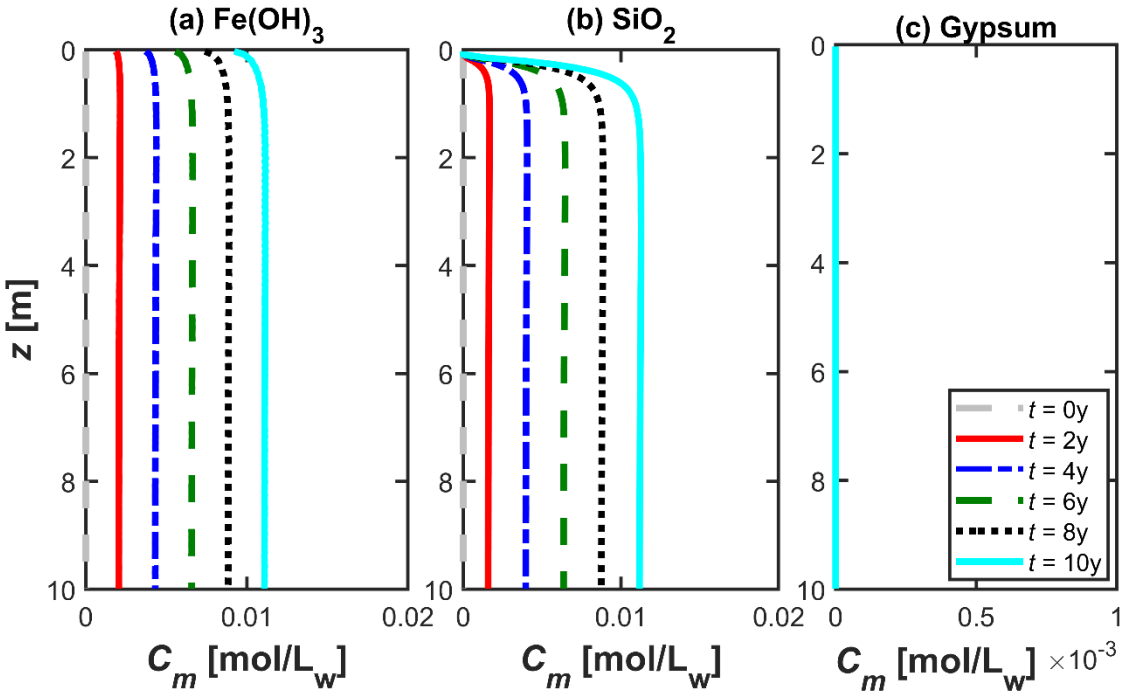

Figure 7: Temporal snapshots of the secondary mineral contents within the simulation domain representing Särkiniemi waste rock pile.

4.2.3 Prediction of the drainage quality from the waste rock pile over a longer time period

Based on the input parameters related to hydraulics, transport, and chemical reactions, this section presents the simulation results for the long-term behaviour of the drainage chemistry from the Särkiniemi waste rock pile. Such simulation scenario can be considered as a simple description of the reactive transport processes within the waste rock pile by considering average properties of the physicochemical parameters. For brevity, Figure 8 plots only the long-term predictions of pH and electrical conductance within the drainage water. These species can be considered as good indicators of acidic drainage conditions.

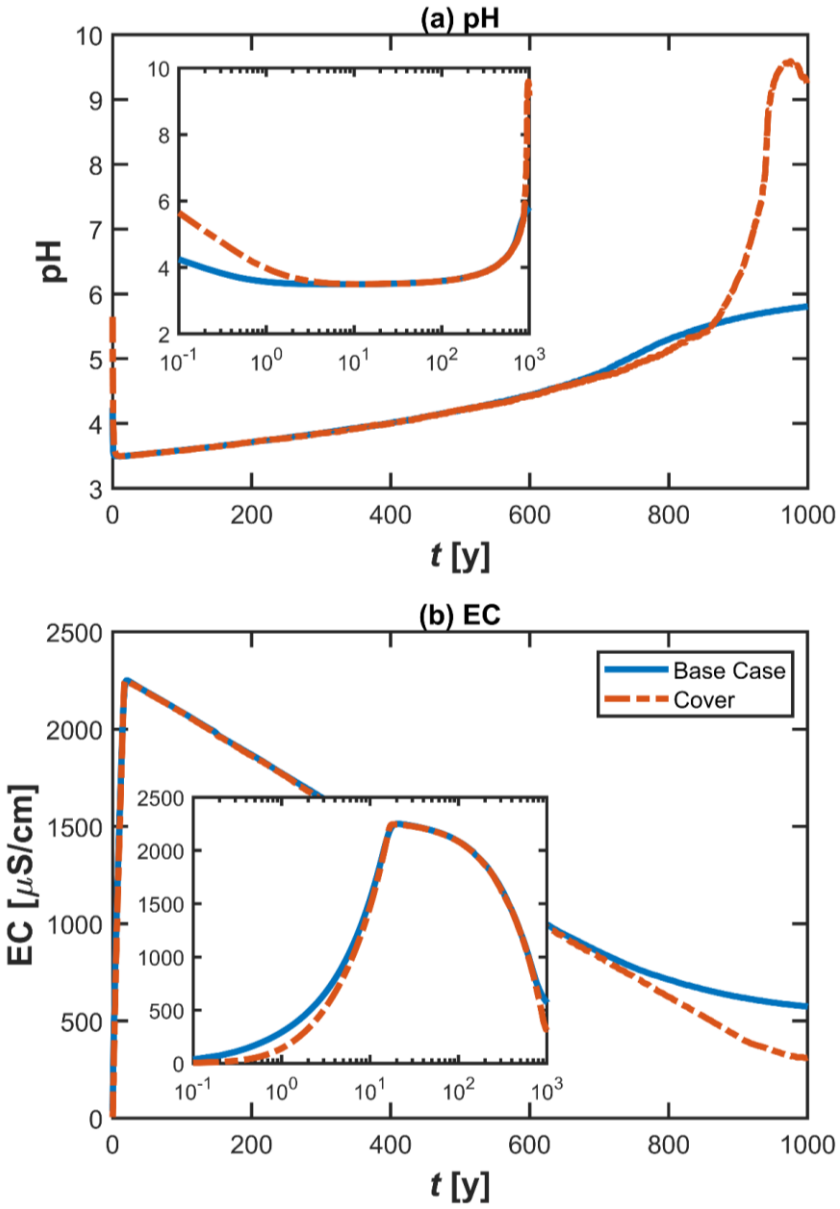

Figure 8: Prediction of the chemical compositions of the drainage water from the Särkiniemi waste rock pile for a period of 1000 years: (a) pH, and (b) electrical conductivity. Figure insets represent the temporal drainage water profiles in semi-log axis to visualize the early the behaviour.

This long-term simulation considered the identical parameters as summarised in Tables 4 and 5, and this simulation scenario is termed as “base case scenario”. The simulation results suggest that the low pH drainage will continue for a very long time (>800-900 years) in this waste facility given the fact that the conditions used in the simulation remains unchanged. The insets in the figure represents the plot in semi-log plot to specifically emphasise the early time

behaviour. Electrical conductivities seem to reach a peak concentration at ~ 10–20 years, which is followed by a uniform decreasing pattern (Figure 8b). This specific time period resembles approximately one pore volume for this simulation domain: i.e. time for a conservative tracer to reach the outlet of the domain. Such behaviour is induced from the fact that with the abundant supply of the oxidant (O_2) the sulphide oxidation mechanisms will occur until all the sulphides are completely exhausted in the waste rock materials. According to the model, the low quality drainage will continue for at least 9 centuries before the complete depletion of the reactive sulphide phases (blue lines, Figure 8). The dissolution mechanisms of the silicate phases appear to be slow to have any significant impact on the buffering of low pH pore water solutions. However, a slowly increasing pattern of pH is clearly observed with increasing time (Figure 8a). Dissolved species resulting from the silicate phases also show a constantly increasing pattern over the time (results not shown).

4.2.4 Prediction of the drainage water quality for the application of covers

Additional analysis for Särkiniemi case was also carried out by performing predictive simulations for scenarios when the waste rock pile is effectively covered with fine grained materials. Application of such covers on the waste facilities will lead to a reduction of the acid generation processes by the limited water flux as well as oxygen ingress into the system. Particularly, in this additional simulation scenario the application of cover was mimicked by applying a recharge rate and gas diffusion coefficient that is only 10% of the original base case scenario's rates (i.e. 10% of the values in Table 4). Figure 8 depicts the predicted drainage pH and electrical conductivities for the scenario under the application of a potential cover (orange lines). It is clear from the figure that the arrival of low pH front is slightly delayed due to the application of a cover (orange line) compared to the base case (blue lines). Such characteristics originates from the limited supply of reactants (i.e. both water and oxygen) that are essential to facilitate the destruction of sulphide phases. The model suggests that the breakthrough of low pH front will occur at ca. 3 years, and an acidic condition will last until ca. 900 years.

The simulation results indicate that the application of a cover does not significantly change the trends of the drainage profiles (Figure 8). This can be explained from the fact that the reaction processes are perhaps not remarkably inhibited in this specific scenario because the oxidation has a relatively stronger control on oxygen concentration, which is supplied by gas diffusion. In order to observe an effective inhibition of weathering processes, gas transport mechanisms should be much reduced compared to the considered extents in this simulation.

4.3 Modelling in Kylylahti Waste Rock Pile

4.3.1 Problem definition and model input

In Kylylahti mine site, predictive simulations were performed by considering a 1-D conceptual model of the waste rock pile in order to predict the vertical propagation of sulphide oxidation, the subsequent mineral dissolution-precipitation front through the waste facility, as well as the

quality of drainage water from the waste pile. The modelled domain was assumed to have a height of 20 m, which is representative of the Kylylahti waste rock pile. The reactive transport simulations were performed by applying a constant water flux boundary at the top of the domain. In addition, the infiltrating water was assumed to have a composition of the generic rainwater for Nordic climate (Reimann et al. 1997) as also used in the simulations of the previous case (i.e. Särkiniemi waste rock pile, Table 6). The net infiltration rate at the inlet was assumed to be 300 mm/y, which is approximated from the net annual precipitation (~626 mm/y) and evaporation (~50% of the precipitation) rate at the study site. In the model, the infiltrating water was also equilibrated with the atmospheric gas content (O_2 and CO_2). For brevity, the domain was assumed to be initially in equilibrium with pure water.

The simulations were performed by considering a uniform Darcy flux throughout the domain without explicitly solving the water flow problem. This assumption was necessary as the detailed information regarding hydrogeology, unsaturated flow conditions, and soil retention curves were not available for this particular site. Nevertheless, such simplified assumption is not too bad especially when the aim is to predict the long-term approximations of the future series of events that would possibly occur in the drainage water (i.e. when the focus is specifically to achieve the right order of magnitude rather than the exact value). Further information regarding the model input parameters used in the simulation for this particular case is provided in Table 7.

Table 7: Geometry, flow and transport parameters used in the simulations of Kylylahti waste rock pile.

Parameters	Values
Domain size (L_z) [m]	20
Discretisation, Δz [cm]	11.42
Time step, Δt [s]	6×10^{6}
Recharge rate, q [mm y^{-1}]	300
Solid density, ρ_s [kg L^{-1}]	2.65
Average porosity, θ [-]	0.50
Diffusion coefficient in aqueous phase, D^w [m^2s^{-1}]	2.00×10^{-9}
Longitudinal dispersivity, α_L [m]	10^{-3}
Diffusion coefficient in gas phase, D^g [m^2s^{-1}]	1.75×10^{-5}
Partial pressures of gas phase at the top boundary	
pO_2 [atm]	$10^{-0.67}$
pCO_2 [atm]	$10^{-3.50}$

As initial mineral contents, the entire simulation domain was assumed to have a homogeneous mineralogical composition characterised by the mineralogical analysis from the waste rock materials. The waste rocks at the Kylylahti Cu-Ni-Co mine site were mainly composed of plagioclase, quartz, and biotite. The waste deposits have a rather high content (>9%) of sulphide bearing minerals, in which pyrite is the main sulphide species with small fractions of pyrrhotite, sphalerite, and pentlandite. Additionally, the waste rock mineralogy include some

fractions of carbonates (~2%), and silicates (~25%) which showed potential acid neutralizing capacity in the lab static tests (cf. also Karlsson et al. 2018). Table 8 depicts the detailed mineralogy of the Kylylahti waste rock materials, and the parameters related to mineral dissolution/precipitation kinetics used in the model. The model considers the minerals listed in Table 8 as primary minerals, whereas ferrihydrite, gypsum, SiO_2 (a), jarosite and gibbsite were allowed to precipitate as secondary minerals. Among the sulphide minerals, the dissolution of pyrite, pyrrhotite, and sphalerite was simulated as kinetically controlled reactions until the equilibrium, whereas pentlandite dissolution was modelled as kinetically controlled irreversible reaction (Table 1).

Table 8: Mineral contents, reactive surface areas of the different minerals, and reaction rate coefficients for the simulations of Kylylahti waste rock pile.

Mineral	**Mineral Content**		**Surface Area, *A***	**Rate Coefficient, *k***	**Reference**
	[wt%]	**[mol L_w^{-1}][b]**	**[$m^2 L_w^{-1}$]**	**[mol $m^{-2} s^{-1}$]**	
Mg-biotite [a]	14.49	0.92	0.05	$10^{-10.97}$	Nagy (1995)
Phlogopite [a]	7.25	0.46	0.05	$10^{-10.97}$	Nagy (1995)
Pyrite	8.79	1.94	1.43[c]	$10^{-10.19}$	Williamson & Rimdstidt
Tremolite	4.92	0.16	0.05	$10^{-8.40}$ (k_1) $10^{-11.98}$ (k_2)	Palandri & Kharaka (2004)
Albite	3.83	0.39	0.06	$10^{-10.16}$	Palandri & Kharaka (2004)
Calcite	1.89	0.50	5[d]	$10^{-1.29}$ (k_1) $10^{-4.46}$ (k_2) $10^{-6.92}$ (k_3)	Plummer et al. (1978)
Pyrrhotite	0.61	0.20	1.43[c]	$10^{-10.19}$	Williamson & Rimstidt (1994)
Sphalerite	0.08	2.17×10^{-2}	1.43[c]	$10^{-9.22}$	Domenech et al. (2002)
Pentlandite	0.05	1.72×10^{-3}	1.43[c]	$10^{-10.19}$	Williamson & Rimdstidt (1994)
Dolomite	0.02	2.87×10^{-3}	5[d]	$10^{-3.19}$ (k_1) $10^{-5.11}$ (k_2) $10^{-7.53}$ (k_3)	Plummer et al. (1978)

[a] Both of these minerals were modelled as the same phase biotite with properties described in Table 1
[b] Moles of mineral per litres of pore water, calculated from the wt% by using a solid density, ρ_s = 2.65 [kg L^{-1}] and an average porosity, θ = 0.50
[c] m^2 of mineral surface area per moles of mineral per litres of pore water
[d] cm^2 mineral surface area per litres of pore water

4.3.2 Evolution of mineralogy in the domain and dissolved elements in the drainage water

The simulated spatial profiles of the mineral contents at different times (t = 0 – 10 years) are illustrated in Figure 9. The top row in this figure (Figure 9a-d) shows the dissolution fronts of the different sulphide minerals representing a sequential depletion of these minerals over time. Such dissolution processes were facilitated by the oxidation reactions of the sulphide minerals with the atmospheric oxygen. The acidic conditions induced by the sulphide oxidation lead to the potential dissolution of the carbonates and silicates in the domain (middle row, Figure 9e-h). It is apparent from the figure that all the calcite is dissolved from the system after approximately 6 years (Figure 9f). Dolomite, on the other hand, was removed almost instantaneously (within < 2 years) because it was present in a small fraction (Figure 9g). Such dissolution fronts of carbonates are realistic as their kinetics are clearly orders of magnitude faster compared to the other mineral kinetics in the system (Table 8).

In contrast, biotite and tremolite dissolve much slower compared to the carbonates as only a very small fractions of these minerals were removed from the simulation domain after 10 years (Figure 9e,h). It is also interesting to notice that the dissolution rate of these silicates was significantly slower at early time (< 6 years) and seems to be accelerated afterwards. This behaviour is surely due to the complex interplay between the acid producing mechanisms from sulphide oxidation and acid neutralizing mechanisms from the carbonates dissolution. Particularly, at early times the pH in pore water is effectively buffered to a near neutral pH range by calcite and dolomite until their complete depletion. Consequently, the dissolution of biotite and tremolite is reasonably slow at this initial period (when calcite and dolomite are present in the domain) as the silicate mineral dissolution usually occurs at low pH. Therefore, the dissolution rate of biotite and tremolite accelerates after ~6 years, when both calcite and dolomite are totally removed from the vertical profile (Figure 9e-h). This phenomena clearly indicates the typical buffering sequence as commonly observed in the acid mine environments (e.g. Blowes & Ptacek 1994, Dold 2010).

The bottom panel of the figure depicts the precipitation of secondary minerals in the system (Figure 9i-l). Precipitation of these secondary minerals was simulated as equilibrium controlled reactions for simplicity. In addition to these four particular minerals shown in the figure, the model also considered the precipitation of amorphous silica and siderite, in which the formation of SiO_2(a) was observed but no precipitation of siderite has occurred (results not shown). The model results reveal that a significant amount of Fe(III) and sulphate species precipitate as ferrihydrite and gypsum phases, respectively (Figure 9i-j). In contrast, the contents of the precipitated jarosite and gibbsite phases are a few orders of magnitude smaller than the ferrihydrite and gypsum phases (Figure 9k-l).

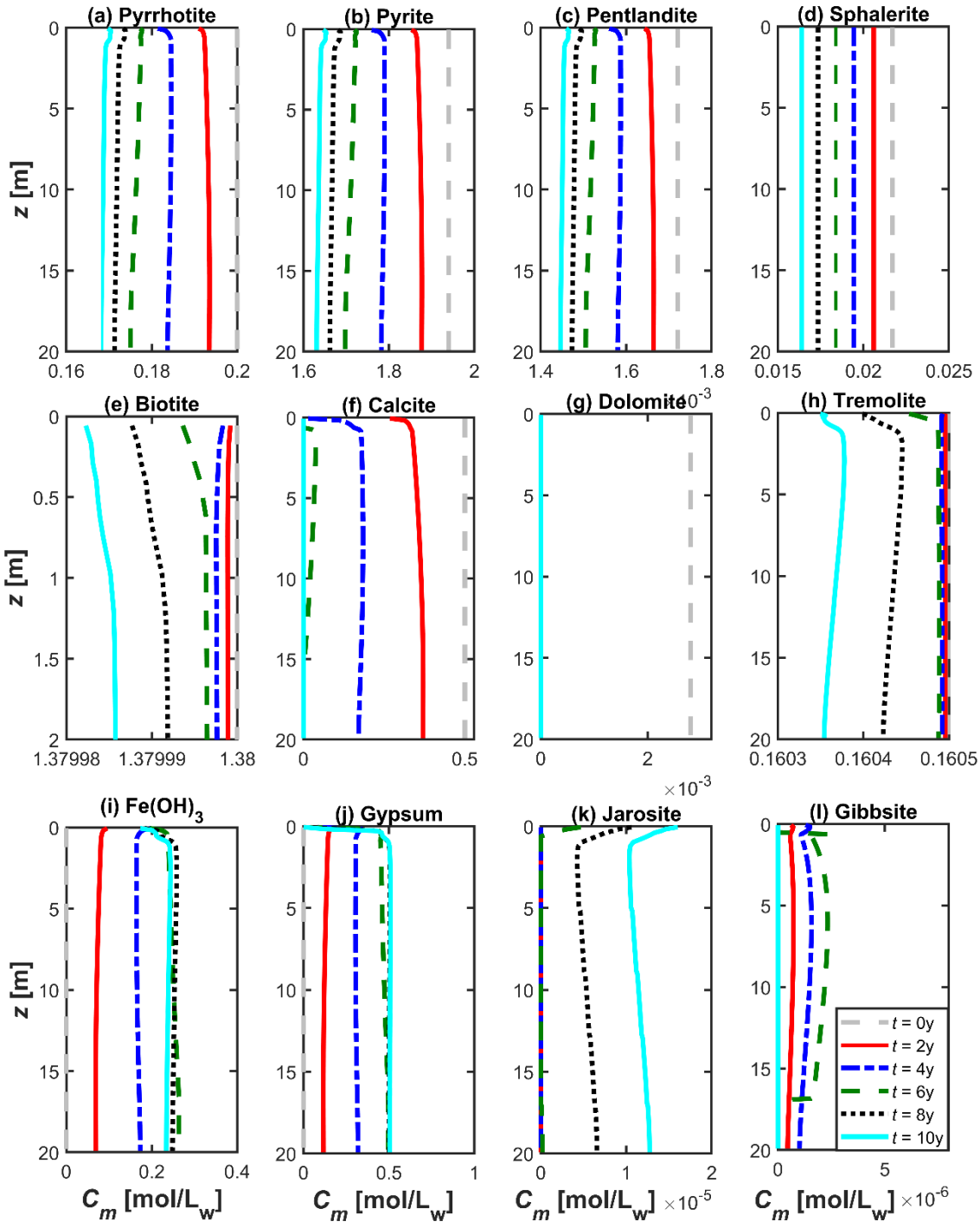

Figure 9: Mineral contents versus depth and their temporal evolution at Kylylahti waste rock pile.

Figure 10 shows the simulated partial pressure profiles of oxygen and carbon dioxide gases into the waste rock pile. These profiles were computed by considering the diffusive transport of gas phases into the waste facility by applying a constant concentration boundary at the top of the domain. After calculating the ingress of gas phases into the domain, the partitioning of O_2 and CO_2 components between the gas and aqueous phases as well as the mineral dissolution-precipitation reactions were computed by PHREEQC (Section 3.4). The simulation results suggest that the gas diffusion is significantly faster compared to both aqueous phase transport as well as the sulphide oxidation reactions as reflected in the vertical profiles in Figure 10. In particular, pO_2 seems to increase quite rapidly in the domain and its spatial profile tends to reach a fairly steady condition after ~3–4 years (Figure 10a).

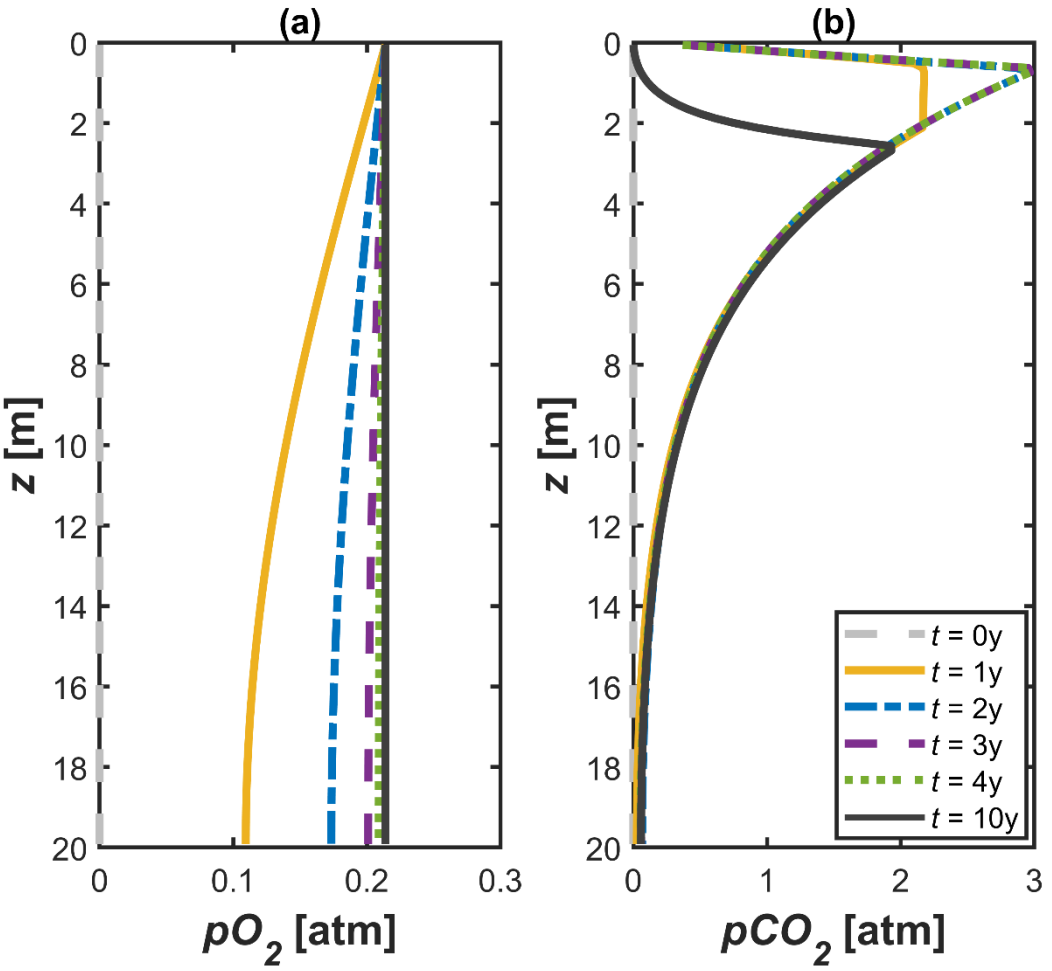

Figure 10: Simulated profiles of gas partial pressures in Kylylahti waste rock pile over depth at selected times: (a) pO_2, and (b) pCO_2.

Simulated values of pCO_2 shows an interesting pattern with a peak value close to the inlet of the domain, where the mineral dissolution reaction rates are the steepest (Figure 10b). Notice that the values of the CO_2 partial pressures are significantly higher (~3 order of magnitudes) compared to the atmospheric condition. Such behaviour and the elevated concentrations are induced from the calcite and dolomite dissolution, which leads to the production of CO_2 gas in the domain. However, pCO_2 starts decreasing with time as all carbonates are depleted after a few years (Figure 9f,g) and as the produced CO_2(g) diffuses out of the waste rock pile towards both the top and bottom boundary (Figure 10b).

Figure 11 summarises the predicted concentrations of the dissolved elements in the drainage water from the waste rock pile. According to the simulation with the literature values as presented in Tables 7 and 8, the pH of the drainage water appears to be in the circumneutral range for a period of approximately 6 years, after which a sharp drop in the pH values occur (blue line, termed as “base case”, Figure 11a). This high pH plateau at the early times can be explained from the equilibration with calcite and dolomite as well as the produced CO_2(g) in the system. However, there is a discrepancy between the modelled profiles (blue lines) and the measured profiles (red markers) at the outlet of the Kylylahti waste rock pile. In particular, the measured profiles show an early breakthrough (red markers, Figure 11a) of pH in the drainage water compared to the modelled temporal pH profile (blue solid line, Figure 8a). This is a scenario that particularly highlights the importance of the site-specific physicochemical parameters required for the accurate predictive modelling. However, this discrepancy in the pH profile can be minimised by increasing the oxidation rate for sulphide dissolution reactions. The dotted orange lines in the figure represent the results from an additional simulation, where a higher oxidation rate was considered by using ca. twice the reactive surface area for sulphide minerals compared to the base case (Table 8).

This case seems to result in a breakthrough time of the low pH front in the drainage water similar to that of the measured values (Figure 11a). The concentrations of SO_4, Ni, Zn, and Fe, i.e. oxidation products of pyrite, pyrrhotite, pentlandite, and sphalerite, show an increasing trend as the mineral dissolution reactions progress (Figure 11b-e). Dissolved concentrations of Fe and SO_4 species are limited by the secondary precipitation of $Fe(OH)_3$(a), jarosite, and gypsum as described in Figure 10. The concentrations of Ca, Mg, and CO_3 are plotted in the primary *y*-axis of Figure 11f, whereas Si, Al, and K are plotted in the secondary *y*-axis. Ca and K show a steady concentration plateau until ~6 years (i.e. time for the low pH breakthrough) followed by a decreasing trend due to the precipitation of gypsum and jarosite phases, respectively. The drainage water contains a significant amount of CO_3 species until all the carbonate phases are exhausted. Mg, Al, and Si concentrations seem to follow an increasing trend with time for the presented simulation duration.

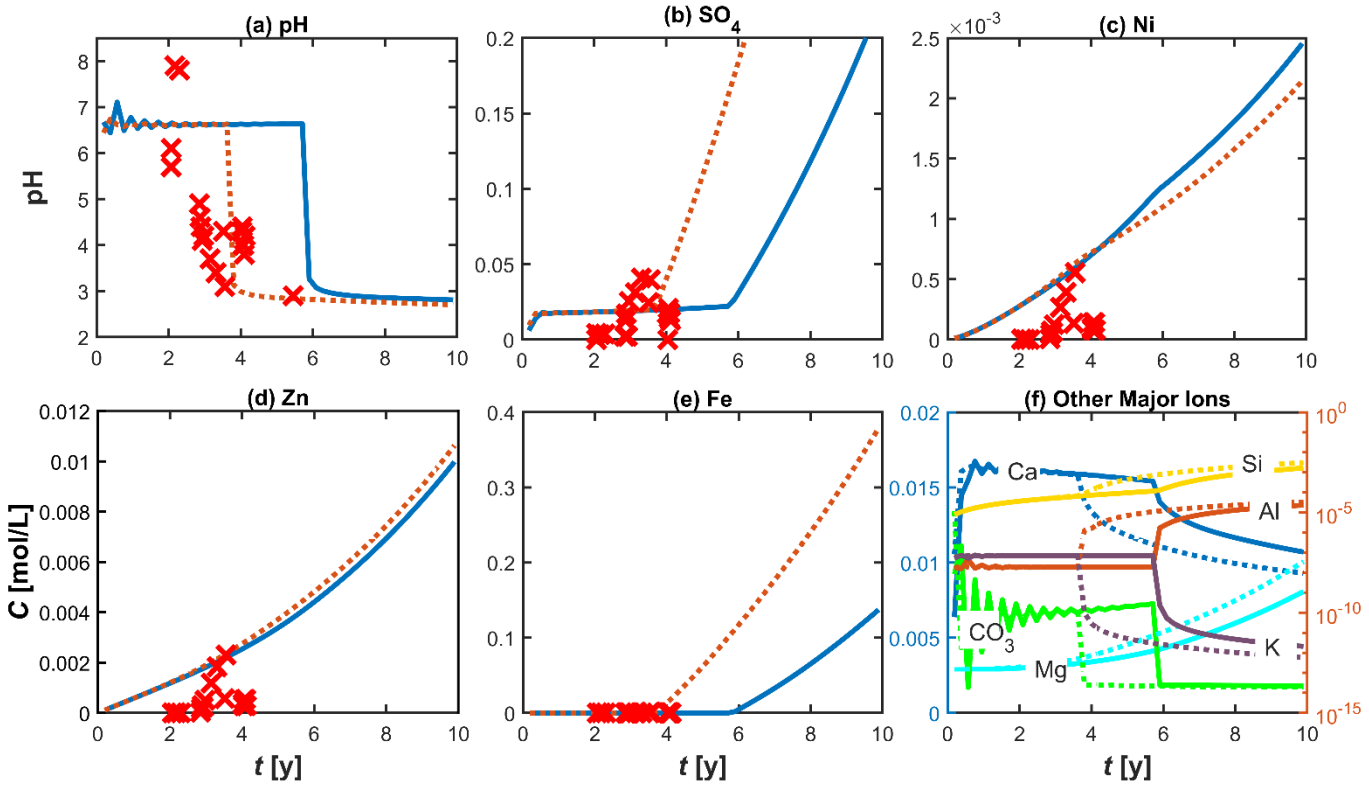

Figure 11: Aqueous concentrations at the drainage of the Kylylahti waste rock pile: (a) pH, (b) SO_4, (c) Ni, (d) Zn, (e) Fe, (f) Ca, Mg, CO_3 (primary *y*-axis), Si, Al, K (secondary *y*-axis). Lines represent the simulated concentrations, whereas the markers represent the measured concentrations in the drainage water. Note that the solid lines are obtained using a reactive surface area of 1.43 m^2/mol mineral (corresponds to a spherical crystal size of 100 μm diameter for the reactive mineral) and the dotted lines are computed with a reactive surface area of 2.43 m^2/mol mineral.

Some extent of discrepancy still exists between the simulated (both blue solid lines and orange dotted lines) and measured values (markers) especially in the detailed features of the pH and other concentration profiles. Such mismatch is originated from the fact that the conceptual model used in these simulations is based on a too simple description of the real system and the available information is too little to rigorously capture all the important processes occurring within the domain or to set accurate boundary and initial conditions. This implies that the predictive simulations were performed in a system that is only partially understood. In order to accurately track the sources of these errors between the model and the data, further site specific information characterising the unsaturated flow, heterogeneities, spatial concentration profiles, as well as reaction kinetics is required to develop a more detailed and sophisticated conceptual model of the waste rock pile. In particular, data related to heterogeneity in hydraulic

conductivities and mineral compositions, oxidation kinetics, reactive surface area, water migration pathways through the waste rock pile, seasonal fluctuations in recharge rate, water saturations, and the extent of gas ingress into pile are needed to resolve these mismatches, confirm hypotheses regarding different processes, as well as to enhance the accuracy of the predictive calculations. Another important thing would be to obtain information about the possible preferential flows. Nevertheless, the simulated concentrations for the different aqueous species appear to be in the similar order as the measured drainage compositions (Figure 11a-e). This implies that even though the current model is too simple to capture all the details and the exact trends of the drainage chemistry, it is still able to provide a reasonable description of approximate system dynamics to predict an average behaviour of the drainage water with compositions consistent to the measurements performed in the field site.

4.3.3 Predictive analysis of the long-term drainage behaviour and sensitivity of the model inputs

Although obtaining a perfect fit with the measured values is beyond the scope of this study, this section extends the analysis of the system behaviour by evaluating the sensitivity with respect to the key model input parameters. This analysis is particularly intended to enhance the system understanding as well to identify the possible improvements in the future data collection that may help increasing the accuracy of the predictions. Figure 12a1-a2 shows the impact of the sulphide oxidation rate on drainage pH profiles. As mentioned earlier, the simulation scenario using the parameters summarised in Tables 7 and 8 was termed as the “base case scenario” (blue lines, Figure 12a1-a2). Two additional simulations were performed by using a: (i) 10-fold higher (“fast kinetics”), and (ii) 10-fold lower (“slow kinetics”) oxidation rate compared to the base case scenario, respectively, and by keeping the remaining parameters identical to the base case. It is evident that a higher oxidation rate (orange dash-dot line) leads to a significantly earlier breakthrough of the low pH front compared to the base case (Figure 12a1).

The situation is opposite for the lower oxidation case (yellow dotted line), where the acidic drainage delays approximately by a factor of ten (i.e. at after 60 years) (Figure 12a1). The simulations performed for a longer time reveal that under the conditions of the base case the acidic drainage at this particular waste rock pile will continue for ~5 centuries before all the sulphide minerals are depleted (blue line, Figure 12a2). In contrast, under the higher oxidation rate, all sulphide phases will be possibly oxidised within ~100 years, after which the drainage pH of the waste rock pile will rise again (dash-dot orange line, Figure 12a2). Notice that the pH at the final plateau for the higher oxidation case is slightly higher than that of the base case within the simulation period. Such behaviour may have induced from the different dynamics and interplay between the calcite and dolomite equilibrium with the sulphide oxidation.

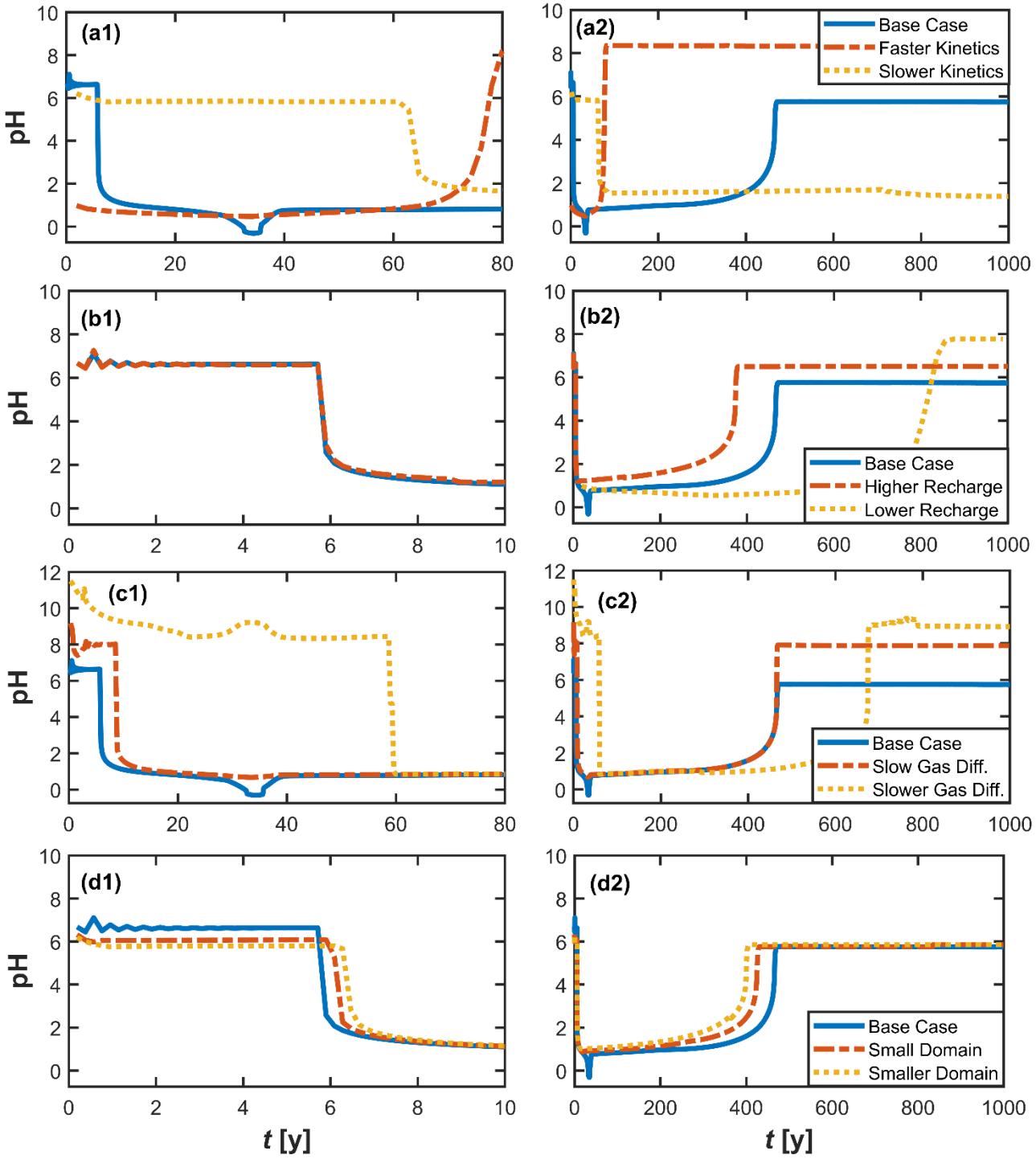

Figure 12: Impact of the model input parameters on the drainage water quality: effects of oxidation rate (a1, a2), recharge rate (b1, b2), gas diffusion (c1, c2), and domain size (d1, d2).

However, under the condition of slower kinetics, the acidic drainage will continue for a rather longer period (dotted yellow line, Figure 12a2). According to the simulation, the sulphides are approximately depleted to 50% of their original contents at the end of 1000 years of simulation.

The second row (b1-b2) in Figure 12 represents the effects of the recharge rate into the waste rock pile. It is interesting to note that the recharge rate does not have a significant impact on the timing of the acid rock drainage (Figure 12b1). In fact the application of a higher (dash-dot orange line) or lower (dotted yellow line) water flux through the domain does not lead to significantly different arrival times of the low pH fronts compared to the base case (blue line). Such phenomena indicates that the early behaviour of the drainage chemistry of this waste rock pile is effectively controlled by the geochemistry rather than the water flow velocity. However, the total duration of the acid mine drainage event is affected by the recharge rate. By applying a 10-fold higher recharge rate (with respect to the base case), the acidic drainage will last for approximately 4 centuries (orange line, Figure 12b2), which is ~100 years shorter compared to the base case scenario (blue line, Figure 12b2). On the other hand, the scenario with a 10-fold lower recharge rate is expected to produce acidic drainage until ~900 years before the sulphidic phases are completely weathered (yellow line, Figure 12b2).

Figure 12c1-c2 shows the impact of gas transport into the waste rock pile. This is particularly evaluated by conducting simulations considering gas diffusion coefficients that are: (i) 10 time smaller (“slow gas diffusion”), and (ii) 100 times smaller (“slower gas diffusion”) compared to the free phase gas diffusion coefficient as used in the base case scenario. The model results suggest that the gas diffusion remarkably influences the timing of the acidic drainage as well as the trends of the pH breakthrough at the end of the waste rock pile. By applying a 10-fold smaller diffusion rate, the temporal pH profiles at the outlet of the domain seem to be very close with only a slight delay (by only a few years) for the slow diffusion case (orange lines) compared to the base case (blue lines, Figure 12c1-c2). The acid mine drainage occurs significantly late (at ~60 years) for the case of 100-fold smaller diffusion coefficient (dotted yellow lines, Figure 12c1). According to the model, the total duration of the acid mine drainage for this particular scenario is around 700 years, which is approximately >200 years longer than in the other two cases (Figure 12c2). Such behaviour is expected because oxygen is one of the key reactants in sulphide weathering processes, and the transport of gas phases eventually determine the effective supply of reactants.

Besides analysing the effects of the input parameters regarding the physical and chemical processes, simulations were also performed to identify the relevance of the geometry of the domain. In particular, these simulations include the use of a: (i) 10 m domain (half of the domain size as used in the base case, “small domain”), and (ii) 5 m domain (one-fourth of the domain size as used in the base case, “smaller domain”). It turns out from the simulations that the total height of the 1-D domain is perhaps the least sensitive parameter among these four parameters described in Figure 12. The use of the shorter domain sizes only slightly delays the arrival of the low front in the drainage water compared to the base case (Figure 12d1). This behaviour is a bit counterintuitive as one would normally expect an early breakthrough for a shorter domain. The time for the total depletion of the sulphide minerals is relatively shorter for the

shorter domains (orange and yellow lines) compared to the geometry of the base case (blue line, Figure 12d2).

None of the conditions and input parameters explored conditions in Figure 12 seem to reproduce the specific patterns of the measured breakthrough curves as shown in Figure 11. This indicates that the possible reason for the discrepancy might not be associated with the input parameters but with the simplicity of the conceptual model. A more representative site-specific conceptual model, capturing all the major mechanisms, is required to accurately reproduce the data. In addition, further information regarding heterogeneity, preferential flow paths, distribution of oxygen concentration or temperature, or details of the measured samples are required to constrain the conceptual hypotheses. For example, the current model considers a homogeneous distribution of the mineralogical assemblages and other physicochemical properties throughout the domain, while it may be likely in the real waste rock pile that the mineralogical compositions are different at locations, where the drainage samples were collected compared to the top layers. In addition, it is also necessary to know the exact locations of sampling and to confirm if the collected drainage water directly passed through the pile or it had followed a partial “runoff” on the pile surfaces. These type of information are crucial to accurately conceptualise different processes in the waste dump systems.

4.3.4 Analysis of the closure scenario for the waste rock pile

This section summarises the impact on the waste rock drainage compositions under the application of a potential cover on the Kylylahti waste rock pile. The application of an effective cover will inhibit the sulphide weathering processes by limiting the penetration of water as well as atmospheric gases into the waste facility (e.g. Tremblay & Hogan 2000, INAP 2009). The condition of the potential cover was mimicked by considering a smaller recharge rate as well gas diffusion coefficient in the simulation. In particular, the presented simulation scenario in Figure 10 was conducted by using a 10-fold smaller recharge rate and a 10-fold smaller gas diffusion coefficient. Basically this scenario resembles a combination of the conditions as presented in Figure 11b-c.

Figure 13 shows a comparison of the predicted pH and SO_4 concentrations in the drainage water for both scenarios representing the base case (blue lines) as well as the case with the application of a cover (orange lines). The front of the acidic drainage is directly correlated with the elevated dissolved concentrations for both scenarios. The figure insets in both plots represent the early time behaviour of the drainage compositions. The modelling results suggest that it will take approximately 4 more years, compared to the base case scenario, for the acidic drainage to occur upon the application of the cover condition used in this simulation (inset, Figure 13a). This also implies that the assumed conditions considered for the cover application do not provide a very effective solution to prevent the acid rock drainage, since the oxygen ingress into the system is not sufficiently inhibited.

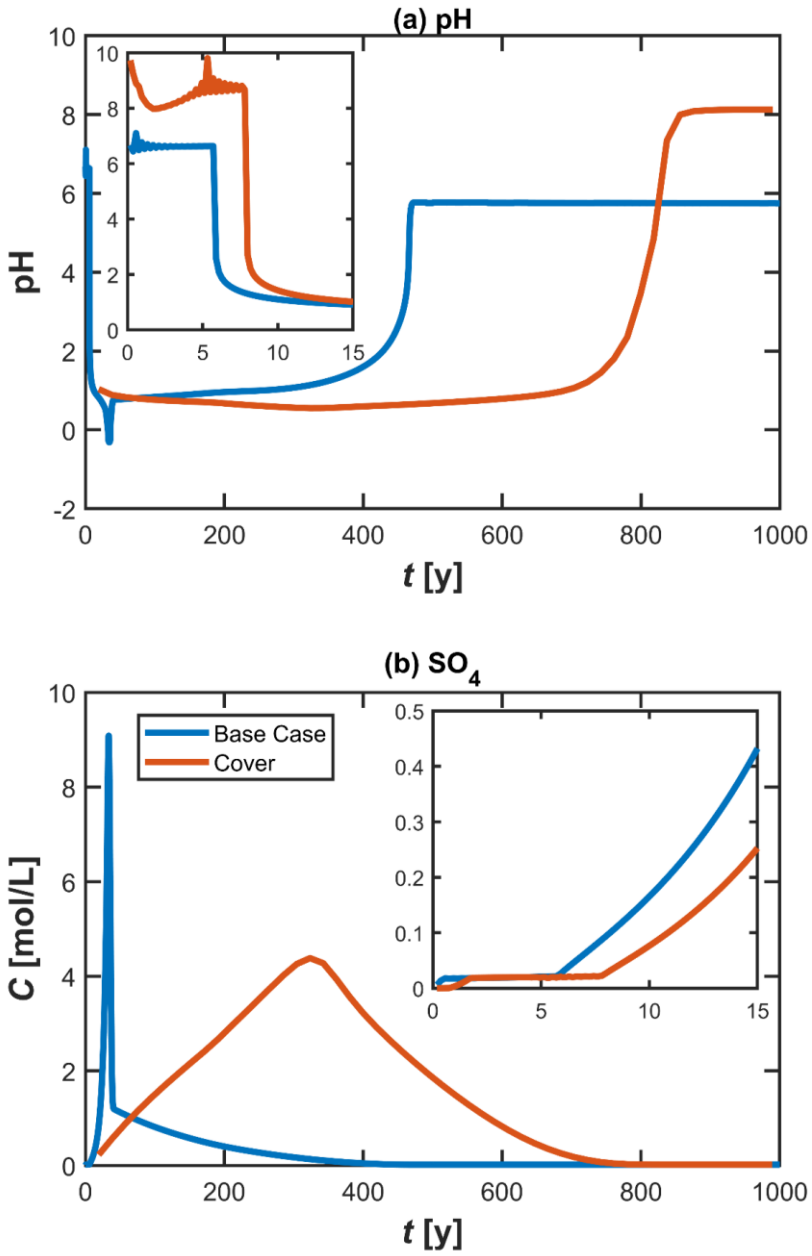

Figure 13: Predicted concentrations of the drainage water at Kylylahti waste rock pile by considering uncovered and covered scenarios for a period of 1000 years. The early time behaviour is highlighted in the inset of each figures.

As pointed out in the previous section (Figure 12c1), for this particular waste rock systems the oxygen penetration rate should be reduced by at least 2 orders of magnitude in order to observe an effective delay of few decades for the acid rock drainage to occur. Therefore, the cover materials and the whole application scheme should be designed in a way that must

ensure very minimal ingress of oxygen into the waste pile. This is also an interesting case that illustrates how predicting modelling can also be effectively used in the design, optimisation, performance analysis of remediation measures (e.g. cover as in this case), risk assessment, and the overall decision making related to the mine waste management.

Sulphate concentrations show different trends in the base case and the cover scenario although the general shapes of these curves are similar (Figure 13b). For the base case scenario, the dissolved SO_4 reaches a peak with extremely high concentrations at ~30–40 years followed by a slow decrease over time. In contrast, the breakthrough curve of SO_4 during the application of a cover results in a more spread profile with a peak concentration that arrives approximately after 4 centuries. The early time behaviour for these scenarios follow a similar trend with a comparatively slower in the drainage concentration for the cover scenario over time (inset, Figure 13b).

The entire duration of the acidic drainage is significantly longer (approximately double) when a cover is applied since the overall extent of sulphide weathering somewhat slows down in this case (Figure 13a). The elevated concentrations of sulphate, which can also be considered as a proxy of acid rock drainage itself, are present in the drainage water until all the sulphidic rocks in the system are fully weathered (Figure 13b). The pH at the final plateau is also slightly different in both cases, which may result from the different levels of interplay between the physical and geochemical processes in the waste rock pile.

4.4 Modelling in Pyhäsalmi Tailings Impoundment

4.4.1 Problem definition and input parameters

This example demonstrates the capability of reactive transport models to predict the drainage quality from a tailings impoundment and the analysis of potential attenuation measures during the closure of the tailings. The simulations were performed in a vertical 1-D unsaturated domain by considering the same mineralogical assemblages as observed in the tailings materials at Pyhäsalmi study site. Such simulation domain can be considered as representative of the unsaturated part of a closed or abandoned tailings impoundment at this particular site. The mineralogical analysis on the samples collected at Pyhäsalmi tailings revealed that the deposits were significantly enriched with sulphide phases (> 31 wt%) with pyrite being the major sulphide mineral (~30 wt%), and relatively smaller fractions of pyrrhotite, chalcopyrite, and sphalerite. The tailings materials contain a smaller fraction of calcite and dolomite. In addition, aluminosilicate mineral phases present at the site include tremolite, biotite, albite, serpentine, K-feldspar, chlorite, anthopyllite, and phlogopite (cf. Karlsson et al. 2018). Based on the mineralogical analysis, a uniform mineral compositions were employed throughout the simulation domain. Table 9 summarises the exact mineral contents used in the predictive simulations. The involved mineral dissolution-precipitation reactions, equilibrium constants, and reaction stoichiometries are depicted in section 3.3.1 (Tables 1-3).

Table 9: Mineral fractions, specific surface areas, and reaction rate coefficients for the simulations of Pyhäsalmi tailings impoundment.

Mineral	Mineral Content [wt%]	Mineral Content [mol L_w^{-1}][b]	Surface Area, *A* [$m^2 L_w^{-1}$]	Rate Coefficient, *k* [mol L_w^{-1} s^{-1}]	Reference
Pyrite	29.9	9.82	1.43[c]	$10^{-8.19}$	Williamson an & Rimstidt (1994)
Hornblende	9.2	1.42	0.50	$10^{-8.11}$	Palandri & Kharaka (2004)
Tremolite	5.0	0.24	0.50	$10^{-8.4}$ (k_1) $10^{-11.98}$ (k_2)	Palandri & Kharaka (2004)
Biotite [a]	3.0	0.29	0.30	$10^{-10.97}$	Nagy (1995)
Albite	1.9	0.29	0.50	$10^{-10.16}$	Palandri & Kharaka (2004)
Serpentine	1.8	0.25	0.05	$10^{-7.08}$	Declercq & Oelkers (2014)
K-feldspar	1.7	0.25	0.50	$10^{-10.06}$	Palandri & Kharaka (2004)
Dolomite	1.7	0.36	5[d]	$10^{-3.19}$ (k_1) $10^{-5.11}$ (k_2) $10^{-7.53}$ (k_3)	Plummer et al. (1978)
Chlorite	1.4	0.10	0.50	$10^{-11.11}$	Palandri & Kharaka (2004)
Calcite	1.1	0.42	5[c]	$10^{-1.29}$ (k_1) $10^{-4.46}$ (k_2) $10^{-6.92}$ (k_3)	Plummer et al. (1978)
Anthophyllite	0.9	0.05	0.50	$10^{-11.94}$	Palandri & Kharaka (2004)
Phlogopite [a]	0.8	0.07	0.30	$10^{-10.97}$	Nagy (1995)
Pyrrhotite	1.0	0.50	1.43[c]	$10^{-8.19}$	Williamson an & Rimstidt (1994)
Chalcopyrite	0.2	0.04	1.43[c]	$10^{-8.19}$	Williamson an & Rimstidt (1994)
Sphalerite	0.1	0.05	1.43[c]	$10^{-9.22}$	Domenech et al. (2002)

[a] Both of these species were modelled as a single component, biotite in the model
[b] Moles of mineral per litres of pore water, calculated from the wt% by using a solid density, ρ_s = 2.65 [kg L^{-1}] and an average porosity, θ = 0.40
[c] m^2 of mineral surface area per moles of mineral per litres of pore water
[d] cm^2 mineral surface area per litres of pore water

Moreover, all relevant oxidation-reduction reactions, gas dissolution-exsolution reactions (partitioning), and aqueous complexation as well as hydrolysis reactions were calculated in PHREEQC using phreeqc database (phreeqc.dat, Parkhurst & Appelo 2013). Modelling was performed by simultaneous oxidation of sulphides as well dissolution of carbonates and silicates. Table 9 illustrates the reactive surface area as well as reaction rate coefficients for individual minerals as used in the simulations. In addition to the primary minerals presented in Table 9, the model also allowed precipitation of goethite, gypsum, jarosite, and siderite as secondary minerals.

In order to simulate the release of the dissolved constituents with the seepage water from the tailings facility, a simulation domain of 2 m was considered (Table 10). This domain can be

assumed as the unsaturated zone located just below the ground surface and on top of the groundwater table in a closed/abandoned tailings impoundment at Pyhäsalmi site. Additionally, this simulation domain can also be representative of both an existing closed tailings impoundment and a potential future tailings facility at this particular study site. A relatively smaller domain size was considered for simplicity as well as to save computational efforts. Since gas transport is pretty fast compared to the other physicochemical processes in the system, the presented modelling formulation requires small time steps to accurately capture different processes and to avoid numerical errors. However, such domain size is still a realistic approximation of the top layers of the unsaturated parts of tailings impoundment. Please note that the top unsaturated layers are usually the most vulnerable zones for the generation of acidic drainage as the oxygen incoming fluxes are the steepest there. Besides, employing a larger domain will not significantly alter the series of events and overall story within the tailings facility, since the same reaction front will continue propagating along the depth. In other words, the calculated drainage chemistry at the end of this 2 m domain can also be viewed as the possible conditions that will possibly occur downstream of 2 m at later times in case the domain size was longer.

Table 10: Geometry, flow and transport parameters used in the reactive transport simulations of Pyhäsalmi tailings impoundment.

Parameters	**Values**
Domain size (L_z) [m]	2
Discretisation, Δz [cm]	2.74
Time step, Δt [s]	1.15×10^{6}
Recharge rate, q [mm y^{-1}]	300
Solid density, ρ_s [kg L^{-1}]	2.65
Average porosity, θ [-]	0.40
Diffusion coefficient in aqueous phase, D^w [m^2s^{-1}]	2.00×10^{-9}
Longitudinal dispersivity, α_L [m]	10^{-3}
Diffusion coefficient in gas phase, D^g [m^2s^{-1}]	1.75×10^{-5}
Partial pressures of gas phase at the top boundary	
pO_2 [atm]	$10^{-0.67}$
pCO_2 [atm]	$10^{-3.50}$

As used in the simulations presented in the previous sections (sections 4.1-4.2) for waste rock piles, a constant recharge condition was used at the top boundary of the simulation domain. The recharge rate (Table 10) was assumed from the net precipitation and evaporation rate at the study site, whereas the compositions of the recharge water was taken from the literature value of generic rainwater composition for Nordic regions (Table 6, Reimann et al. 1997). In order to numerically solve the transport and reaction equations, the simulation domain was discretised into 73 cells (Δz = 2.74 cm), and a time step (Δt) of 1.15×10^{6} seconds was used. Transport of gas phases was simulated by applying constant partial pressures of oxygen and carbon dioxide at the top boundary (Table 10). After updating the gas partial pressures and

compositions at cells of the domain, transport of the aqueous species, mass transfer of gas components between the water and gas phase, and the geochemical reactions were simultaneously solved. As described in section 3.4 that the latter two steps were calculated within the geochemical solver PHREEQC. For the advection of water, a uniform seepage velocity was used in the entire domain. A water saturation (S_w) of 0.20 was arbitrarily chosen in order to calculate the effective transport parameters in water (e.g. D_p^w) and gas (D_p^g) phases within the unsaturated porous matrix. Table 10 summarises all the relevant model parameters used in the simulations.

4.4.2 Drainage compositions from tailings impoundment

Figure 14 shows the predicted pH (blue line) of the tailings facility's drainage as well as the concentrations of the major product (SO_4, orange line) of sulphide minerals as a function of time. According to the simulation, under the considered assumptions it would take approximately 5 years for the acidic drainage to occur at this 2 m unsaturated tailings facility. This delay period is due to presence of calcite and dolomite, which effectively buffer the pore water pH until they are completely dissolved. Such behaviour is also apparent from the early values of pH, which shows reasonably higher pH (~10) followed by a plateau of the circumneutral range (~7.8) until the arrival of the acidic front.

This initial rise in pH can be explained from the equilibrium of the pore water with the carbonate minerals and from the fact that it takes some time for the oxygen (Figure 16) to transport through the domain to initiate sulphide oxidation and subsequent generation of protons. However, as the time progresses, the weathering of sulphide minerals accelerates due to the oxygen ingress into the tailings facility. As a consequence, a drop in the drainage pH occurs although the resultant pH stays slightly over the neutral value until 5 years. This behaviour is surely triggered from a tight interplay between the simultaneous sulphide and carbonate dissolutions and their reaction kinetics. Generally the dissolution rates of calcite and dolomite are orders of magnitude faster than the sulphide oxidation reactions, and such carbonate dissolution mechanisms even accelerate under acidic conditions (Table 2 and 9). Therefore, even though the overall sulphide content is remarkable at these deposits, the acid producing mechanisms from sulphide oxidation cannot overcome the acid neutralizing mechanisms from carbonate dissolution as long as any carbonate mineral is present in the system. For this simultaneous sulphide and carbonate weathering period, the net effect is the buffering of drainage pH to a certain range characterised by the involved carbonate minerals as observed in this simulation.

The hypothesis discussed in the above paragraph can also be verified by looking into the drainage concentration profiles of the major ions in Figures 14 and 15. For instance, SO_4 concentration appears to increase to a peak value at around 4 years after which it decreases until the arrival time of low pH front (Figure 14). This implies that although pH is buffered at this particular time period because of the carbonate equilibrium, the signature of the simultaneous occurrence of sulphide weathering is distinct with the sulphate concentration trends in the drainage water. A similar trend is also obvious in the concentration profiles of Zn (green dash-

dotted line) and Cu (purple dotted line) that are basically the oxidation products of sphalerite and chalcopyrite (Figure 15a).

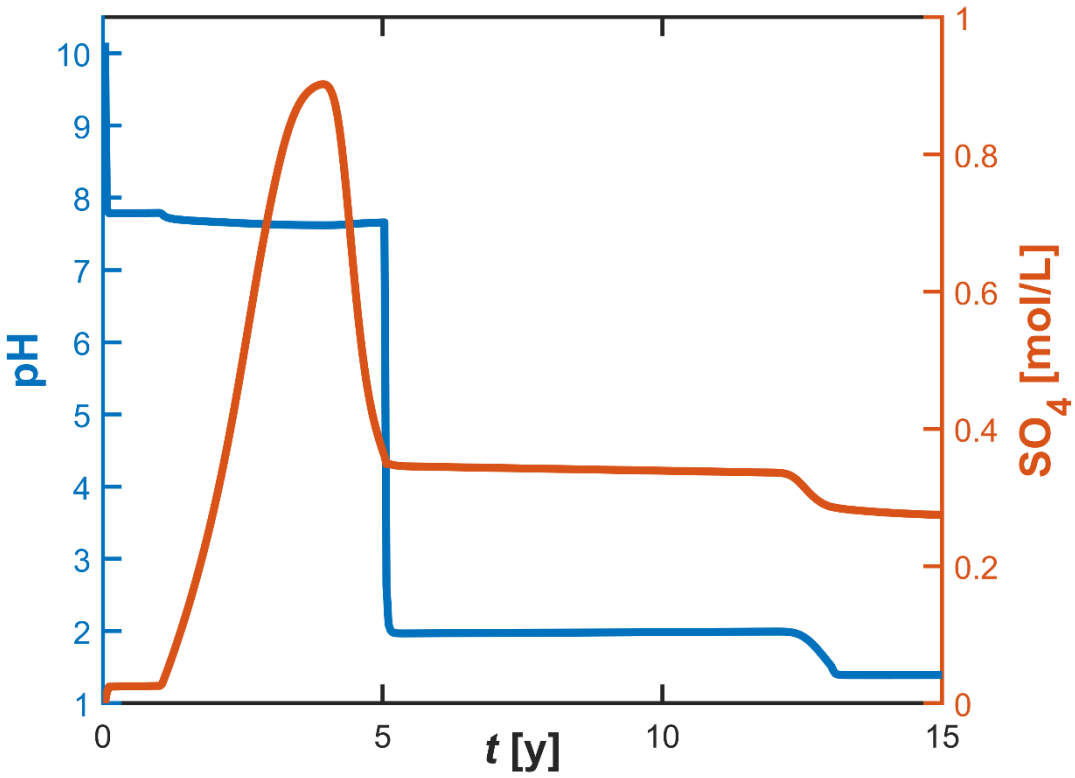

Figure 14: Simulated drainage pH and SO_4 concentrations of pH and from the unsaturated part of a tailings impoundment based on the mineralogy of Pyhäsalmi mine site.

Additionally, the profiles of Ca, Mg, and CO_3 also clearly show the evidence of calcite and dolomite dissolution during this period (Figure 15). Ca concentration (light blue solid line) seems to rise to a peak value almost instantaneously demonstrating a very fast dissolution of calcite at the very beginning of the simulation (Figure 15a). Mg concentration also shows a similar pattern except a delay in the arrival of peak concentration (orange dash-dotted line, Figure 15b). This is perhaps induced from the slightly lower dissolution rate of dolomite compared to calcite. CO_3 concentrations also show consistent patterns indicating that the buffering mechanisms of carbonate phases take place until ~5 years (blue dotted line). Total Fe concentrations in the effluent water is reasonably low compared to sulphate species as Fe is attenuated by the formation of iron-oxyhydroxide phases at the active oxidation front (blue solid line, Figure 12b). Also, notice that the simulated concentration profiles of SO_4 and Mg show a very similar shape and significantly higher concentrations (~1 mol L^{-1} at the peak) than

that of the other oxidation products. This behaviour perhaps indicates that there might be precipitation of additional secondary mineral phases involving Mg and SO_4 that are currently not included in the model. This can probably also explain the higher simulated concentrations of these species compared to the measured values in seepage water as depicted in Table 11.

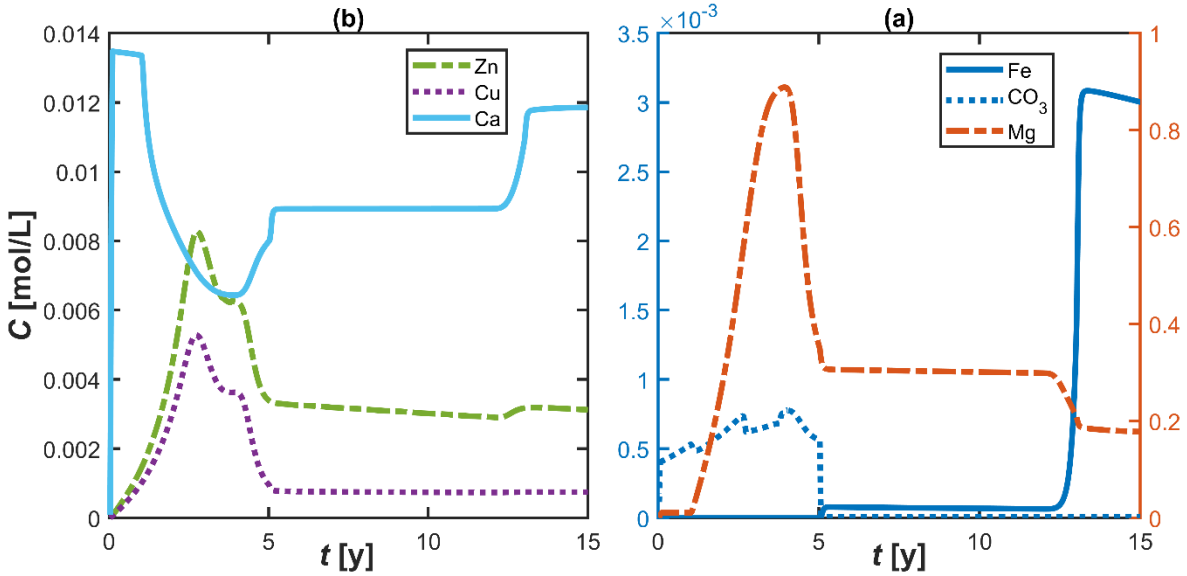

Figure 15: Predicted aqueous phase concentrations in the drainage water from the Pyhäsalmi tailings impoundment: (a) Zn, Cu, and Ca, (b) Fe, CO_3 (primary *y*-axis), and Mg (secondary *y*-axis).

After 5 years of simulation time, the drainage water reaches a second low pH plateau when all the strongly buffering carbonate minerals are removed from the domain (Figure 14 and 17e-f). The pH value at this late time plateau is ~2, which is slightly lower than the measured pH (2.87, Table 11) at the seepage water in the corresponding tailings pond (section 2) where the tailings samples were collected. Table 11 shows the measured concentrations of different dissolved elements in the seepage water. In addition, this predicted pH at late times, as shown in Figure 11, also shows a good agreement with the NAG pH (2.14) that was experimentally determined by the laboratory based NAG test using the tailings materials (cf. also Karlsson et al. 2018). Concentrations of other sulphide oxidation products such as SO_4, Zn, Cu also follow a similar trend as observed in the pH profile, whereas dissolved Fe concentration is significantly dominated by the secondary mineral phases. Ca concentration is also clearly limited by the precipitation of gypsum and jarosite phases.

Table 11: Chemical composition of the seepage water in the tailings at Pyhäsalmi site.

Species	Conc. [mol L^{-1}]	Species	Conc. [mol L^{-1}]	Species	Conc. [mol L^{-1}]
Fe(II)	1.23×10^{-8}	Sb	1.64×10^{-8}	Mn	1.91×10^{-4}
Ag	6.44×10^{-12}	Se	3.53×10^{-7}	Mo	5.39×10^{-8}
Al	8.93×10^{-4}	Sr	1.36×10^{-5}	Ni	1.59×10^{-6}
As	2.91×10^{-7}	Th	$1{,}01\times10^{-8}$	P	5.91×10^{-6}
B	9.11×10^{-6}	Tl	3.40×10^{-12}	Pb	2.22×10^{-9}
Ba	1.54×10^{-8}	U	4.09×10^{-7}	Rb	$9{,}78\times10^{-7}$
Be	2.96×10^{-7}	V	5.19×10^{-7}	Si	1.05×10^{-3}
Bi	1.11×10^{-7}	Zn	3.70×10^{-4}	Br	8.69×10^{-9}
Cd	3.33×10^{-8}	Ca	1.1310^{-2}	Cl	1.69×10^{-3}
Co	3.21×10^{-6}	Fe	1.70×10^{-2}	F	1.74×10^{-4}
Cr	2.42×10^{-7}	K	3.17×10^{-4}	NO_3	2.24×10^{-8}
Cu	478×10^{-6}	Mg	2.06×10^{-2}	SO_4	5.21×10^{-2}
I	5.80×10^{-7}	Na	3.05×10^{-3}	pH	2.9
Li	4.61×10^{-5}	S	5.68×10^{-2}	EC[a]	643.70

[a] in [mS/m]

4.4.3 Gas phase transport and evolution of minerals within the domain

Transport of the gas phases was simulated at the Pyhäsalmi tailings by considering only the diffusion of the gas components. In particular, the simulations were performed by considering a “semi-open condition”, which assumes a connection to the outside atmosphere providing an unlimited supply of oxygen at the inlet boundary. Such assumption mimics the unsaturated conditions of the tailings and gas diffusion is characterised via the pore diffusion coefficient. Figure 16 shows the simulated partial gas pressures as well as compositions in the tailings facility at given times. The model results reveal that the gas compositions are continuously changing as the time proceeds. For instance, up to 2 years higher oxygen partial pressures (i.e. close to the atmospheric value) only exist at the very shallow depth of the domain (Figure 16a). As the sulphide minerals start depleting, the oxygen front also penetrates deeper into the domain. The gas phase concentration of O_2 also shows a similar pattern that is directly correlated to the partial pressures (Figure 16c).

According to the simulations, it takes more than 5 years for the O_2 to achieve a close-to-saturation condition, with respect to atmospheric composition, in the tailings facility. It is interesting to note that such timing is also consistent with the arrival of the low pH drainage as shown in Figure 14. Carbon dioxide concentrations are mainly controlled by the dissolution of calcite and dolomite. pCO_2 values seem to achieve a close-to-atmosphere condition pretty fast as illustrated in Figure 16b. In contrast, the simulated vertical profiles of the CO_2(g) concentrations suggest that a much higher values are present in the system compared to the atmospheric content (Figure 16d). Such behaviour indicates that carbon dioxide is produced in the tailings as a result of calcite and dolomite dissolution. Initially,

relatively uniform higher compositions of CO_2(g) are observed throughout the domain (blue and orange lines, Figure 16d), while it starts depleting with time as CO_2(g) diffuses out of the system (yellow, green and purple lines, Figure 16d). Carbon dioxide contents drop quite fast in the unsaturated domain once the system is completely exhausted with respect to the carbonate minerals.

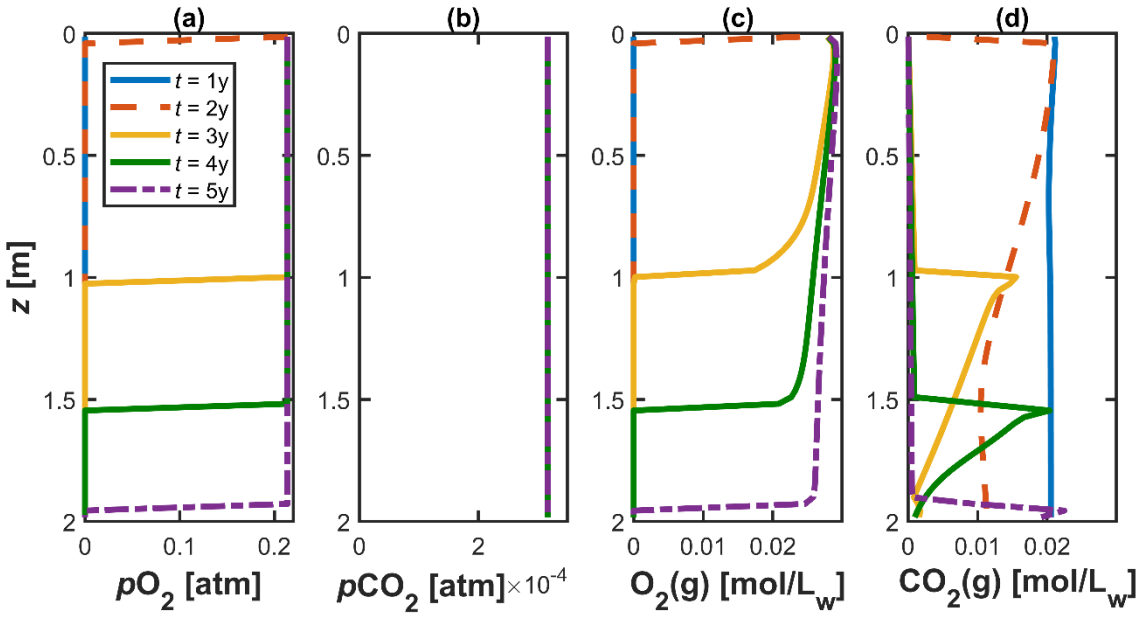

Figure 16: Modelled spatial profiles for the partial pressures (a, b) and gas phase compositions (c, d) of O_2 (a, c) and CO_2 (b, d) at different times.

Figure 17 illustrates the temporal snapshots of the mineralogical assemblages within the tailings impoundment at different selected times. For brevity, only the sulphide and carbonate mineral profiles are shown in this figure as they are the major primary minerals controlling the system behaviour. Additionally, only the profiles of goethite and gypsum were plotted in this figure among the secondary minerals. It is clear from the figure that as the oxygen penetrates deeper into the tailings, the sulphide phases start depleting (Figure 17a-d). The oxidation fronts of these minerals are clearly more prominent close to the inlet, where the gradients of the oxygen mass fluxes are the highest. Pyrite, pyrrhotite, and chalcopyrite profiles follow a similar trend, whereas sphalerite profiles are slightly different indicating a relatively uniform extent of dissolution throughout the domain. This happens because sphalerite kinetics was modelled with the rate law obtained from Domenech et al. (2002), which describes the oxidation rate only as a function of pH without considering any explicit relation with O_2 concentration (Table 2). At the end of 10 years the overall depletion of the sulphide minerals is roughly below 10%.

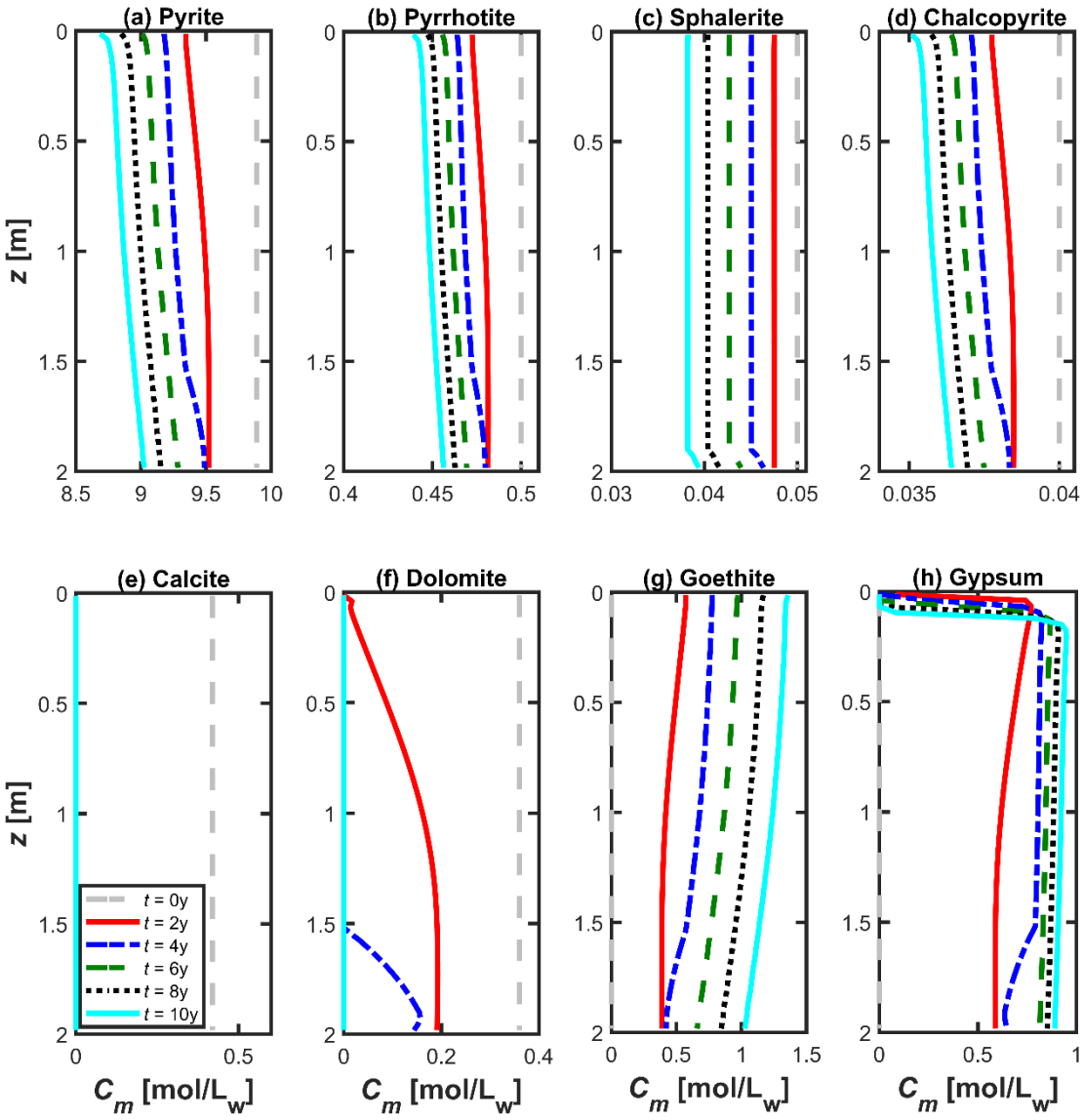

Figure 17: Profiles of the mineral contents at Pyhäsalmi tailings impoundment over vertical distance. Different colours resemble the profiles at different times.

The model predicts that for this particular scenario and under the simulation conditions calcite will completely dissolve within < 2 years (Figure 17e). In contrast, dolomite will take slightly longer (~4-5 years) to be depleted from the system (Figure 17f). The early time (0-5 years) pH in the drainage water (Figure 14) is solely controlled by the dissolution mechanisms of these two minerals. Figure 17g shows the precipitation of goethite over time. Goethite formation limits the dissolved iron concentrations in the pore water as well as it enhances the acidic conditions (Dold 2010). Such phenomena is consistent with the predicted Fe concentrations in the

drainage water (Figure 15b). Figure 17h illustrates the profiles of secondary gypsum minerals, which eventually attenuate dissolved Ca and SO_4 concentrations from the pore water. This also explains the comparatively lower concentration of Ca with respect to Mg in drainage water (Figure 15), although both of these species mainly produce from the calcite and dolomite dissolutions. Moreover, Mg can also result from the Mg silicate phases such as serpentine. It is also clear from Figure 17h that the formation of gypsum is relatively faster at the early times when carbonates are still present in the system. After ~5-6 years, the increase in gypsum content is very low as the system lacks one of the major sources of Ca when all carbonates are fully removed. SO_4 concentration is also effectively attenuated by the gypsum precipitation but the pore water still contains significantly higher concentrations of sulphate and Mg indicating the potential for the precipitation of other secondary phases.

4.4.4 Long-term behaviour of the drainage water from the tailings impoundment

Figure 18 illustrates the prediction of the drainage water quality from the tailings impoundment for a longer period of time (100 years). The simulation results suggest that acidic drainage will continue for centuries under the conditions summarised in Tables 9 and 10 (base case, blue lines, Figure 18a). pH at the drainage water at the late times (>15 years) seems to be quite stable. However, a closer inspection reveals that pH, in fact, very slowly increases over time (Figure 18a). This is due to the dissolution of the silicate minerals, which is essentially facilitated by the low pH conditions. However, the overall influence of silicate weathering on the drainage pH is very small due to their slow kinetics. According to the model, it would take several centuries for the aluminosilicates to increase the effluent pH to a noticeable limit.

In fact, given the mineralogical compositions for this particular materials, silicate weathering processes may never be able to rise the drainage pH to a circumneutral range especially when sulphides are still present in the domain. The sulphate concentrations also follow a similar trend with a very slow decrease at the late times (blue line, Figure 18b).

Besides the base case scenario (i.e. simulation using the parameters of Tables 9 and 10), additional simulations were also performed to analyse the effects of the sulphide oxidation rates on the long-term drainage quality. These simulations include the use of: (i) a 10-fold higher sulphide oxidation rate (“fast kinetics”, yellow dash-dotted lines), and (ii) a 10-fold lower sulphide oxidation rate (“slow kinetics”, orange dotted lines) compared to the oxidation rate used at the base case simulation.

The simulation results suggest that a higher oxidation rate for sulphides does not have significant impacts, compared to the base case, on the timings of the arrival of low pH fronts and SO_4 concentrations (yellow lines, Figure 18). However, under higher reaction rate the breakthrough patterns of SO_4 is different with the profile being more spread and a relatively higher peak concentration. On the contrary, drainage pH follows a different trend (orange dotted line, Figure 18a) when the simulation was performed by applying a lower oxidation rate for the sulphide minerals, while keeping all the other parameters identical as in the base case. For this case, the high pH plateau (~7.8) continues for a much longer period (~20 years)

compared to the base case. Afterwards, an additional plateau of pH = ~4 is observed which ranges from *t* = ~20–50 years (Figure 18a). Finally, the pH of the drainage water drops to around 3, which will probably continue for a rather long time. SO_4 concentration profile is also significantly different for this case of lower dissolution of sulphides (orange dotted line, Figure 15b). Particularly, the peak concentration is smaller by roughly an order of magnitude relative to the base case. The arrival time of the SO_4 breakthrough for this particular case is also delayed compared to the other two cases.

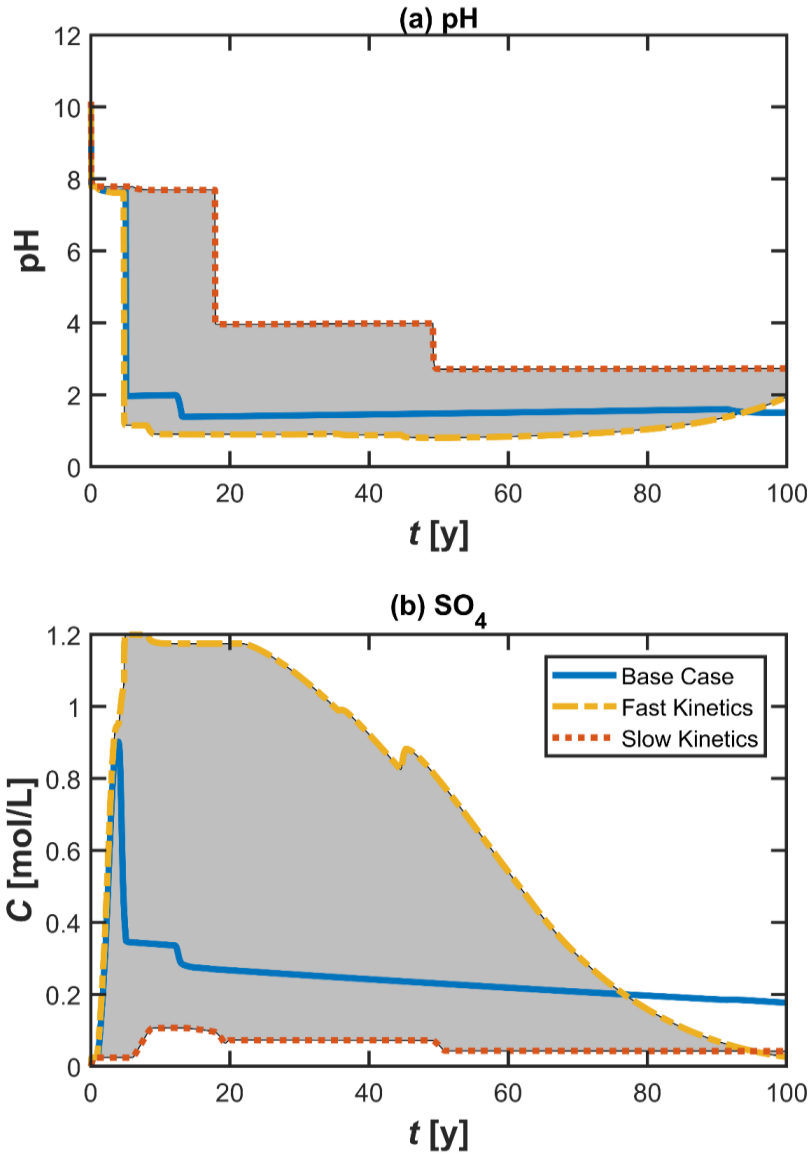

Figure 18: Predicted long-term behaviour of pH (a) and SO_4 (b) concentrations in the drainage water from the proposed tailings impoundment at Pyhäsalmi site: blue solid line–base case (A=1.43 $m^2mol^{-1}L_w^{-1}$), orange dotted line–lower oxidation rate (A=0.143 $m^2mol^{-1}L_w^{-1}$), and yellow dash-dotted line–higher oxidation rate (A=10.43 $m^2mol^{-1}L_w^{-1}$).

The differences in the drainage chemistry in these three cases are driven by the complex interplay between all the physical and geochemical processes occurring in the system. This outcome also reveals that the specific condition of a drainage is ultimately determined by the relative contributions of these involved collective processes rather than a single process. In fact, the acid mine drainage problem is a flux-driven process, where all the different physicochemical processes simultaneously play their own parts towards the overall outcome. Therefore, it is of utmost importance to properly characterise the involved mechanisms in order to accurately predict the drainage water quality as well the system dynamics. The grey area in Figure 18 indicates the area of influence of the drainage behaviour associated with the sulphide oxidation rates. This implies that the drainage pH as well as the elevated dissolved concentrations would fluctuate within this range due to the change of sulphide mineral dissolution kinetics by two orders of magnitude. This is also an example that demonstrates the importance of accurately characterising the oxidation kinetics of sulphide minerals. This grey area can be narrowed down by obtaining the data regarding the sulphide dissolution kinetics by means of kinetic tests (e.g. humidity cell tests or column tests) with the waste materials (e.g. Maest & Nordstrom 2017).

4.4.5 Effects of the application of a cover on the tailings impoundment

This section illustrates the prediction of the drainage quality from the tailings impoundment upon the application of a potential cover on top of the Pyhäsalmi waste facility during a closure scenario. In the reactive transport simulations, the cover conditions were mimicked by employing a lower (10-fold) recharge rate as well as gas diffusion coefficient. Such treatment is reasonable as the application of cover materials will not only inhibit the oxygen ingress into pile but also limit the water penetration into the tailings facility (e.g. Tremblay & Hogan 2000, INAP 2009). In this simulation, the cover is applied from the start of the tailings disposal. Figure 19 shows the predicted pH and SO_4 concentrations in the drainage water for both the base case (light green solid line) and the cover scenario (dark red dash-dotted line) for a period of 1000 years.

The model predicts that it would take around four centuries (as indicated in the low pH conditions) for the sulphide minerals to be completely depleted from this relatively short 2 m domain under the “semi-open conditions” as used in the base case simulation (Figure 19a). This behaviour is expected as the waste deposits are extremely enriched with the sulphide phases, especially pyrite (Table 9). SO_4 concentrations, which can be regarded as a proxy for the elevated dissolved concentrations indicating acid mine drainage, also follow a consistent pattern showing relatively higher concentrations up to ~400 years before dropping down close to zero (Figure 19b).

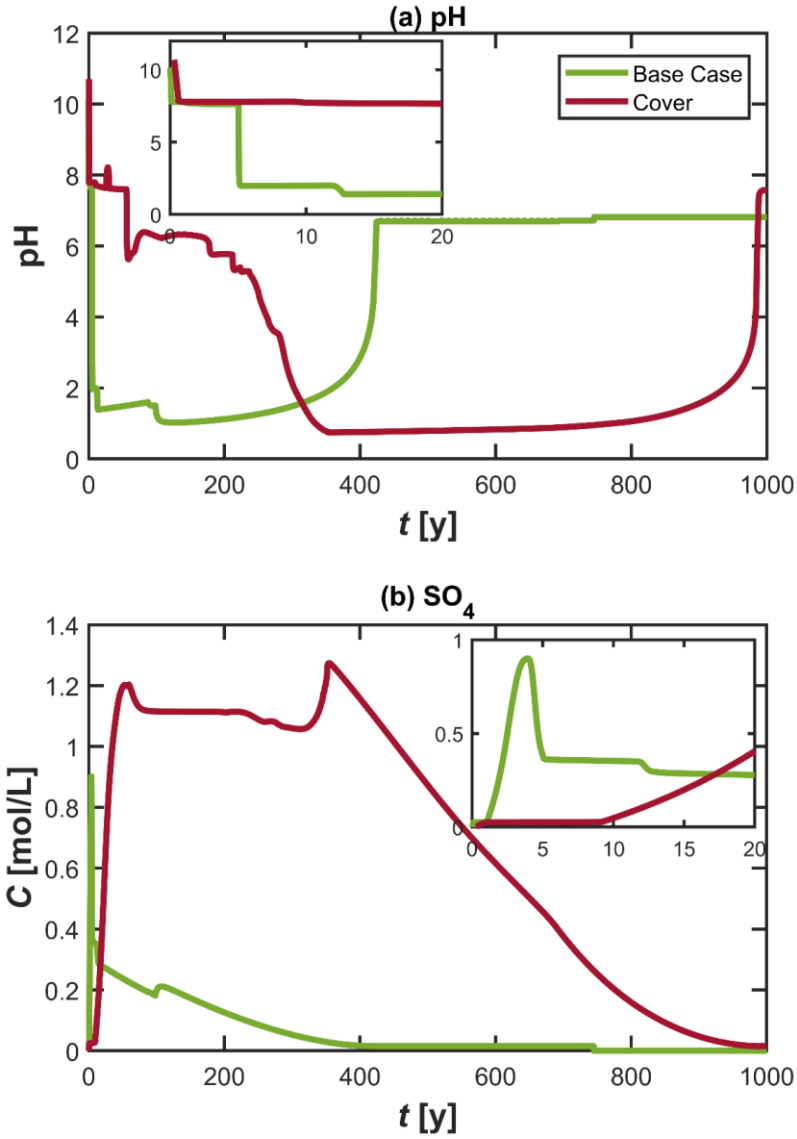

Figure 19: Prediction of the long-term behaviour of drainage water quality from the tailings impoundment at Pyhäsalmi site by considering the application of a potential cover on the tailings facility.

The situation is different upon the application of a potential cover on the tailings facility. Due to the reduced penetration rate of the recharge water and lower supply of oxygen in the tailings, the drainage pH stays higher for a longer period (t = ~0–80 years) at the beginning of the profile under the cover condition compared to the base case (Figure 19a and figure inset). Afterwards, the drainage pH stays around 6 for almost another two centuries (dark red dash-dotted line, Figure 19a), before it drops to acidic conditions (pH < 2). This early time buffering for the couple of 100 years is probably due to a combined effect of the limited supply of the reactants (i.e.

water and oxygen) into the system for the sulphide oxidation reactions as well as the equilibrium of the carbonate minerals. Dissolved sulphate concentration also seems to be stable around this pH buffering region as shown in Figure 19b (dark red dash-dotted line). The simulations also predict that even though the acidic drainage will not occur before ~400 years, when a potential cover is applied on the tailings, the net duration of the acid mine drainage will be comparatively longer for this condition relative to the base case (Figure 19a). According to the model, for the closure scenario, sulphide weathering will take place until ~1000 years, when all the sulphide phases are completely removed from the domain. In contrast, SO_4 concentrations show a decreasing pattern during the acidic drainage events (t = ~400–1000 years) before dropping to zero.

4.5 Uncertainties in the predictions

The simulation results presented in the above sections were based on the conceptual models developed mainly from the mineralogical data collected in each study site. In addition, further information were also available such as concentration measurement in the drainage water, acid production or neutralisation potential of the waste materials from the laboratory based static tests, and elemental concentrations of the waste deposits from e.g. XRF analysis. These information also helped constraining the conceptual and numerical model towards some extent of realistic basis for individual waste facilities. However, the presented predictive analyses still rely on a lot of assumptions and literature values for the model input parameters. There was not enough information regarding the water flow, solute and gas transport, moisture content/water saturation profiles, porosities, permeability, and heterogeneity. Therefore, it is only foreseeable that the prediction results presented in this study contain different levels of uncertainties. The major sources of uncertainties for these particular presented cases can be briefly summarised as the following:

- *Heterogeneity:* In the simulations, a uniform mineralogical composition was assumed for the whole simulation domain. However, this is not always a realistic assumption as heterogeneity is a phenomenon that exists in any sort of geological media. The mineralogy in different parts of the waste facility may contain different mineral fractions, which is not included in the model. This might be particularly true for Kylylahti waste rock pile example, where the historical drainage pattern does not completely match with the model results. In addition to the mineralogy, heterogeneity can also be relevant in other chemical, hydraulic (e.g. hydraulic conductivity, permeability, porosity), and transport properties (e.g. seepage velocity, local dispersion). Therefore, a representative description of the heterogeneity for the whole study area is crucial for a meaningful prediction.
- *Water saturation and moisture content:* The presented simulations did not solve the water flow through the domain. Flow problem was treated by employing a constant seepage velocity throughout the entire domain. In unsaturated systems, water flow is

controlled by several factors including water saturation, capillary pressure, specific storage, and relative permeability. Explicitly measuring the saturation profiles along the domain would significantly improve the conceptual model.

- *Preferential flow:* All the simulations presented in this study were conducted by explicitly considering the flow and transport in typical porous media and by ignoring any preferential flows. The presence of any preferential flow paths can remarkably change the prediction outcomes. The presence and distribution of possible preferential flow paths is an important aspect that must be experimentally confirmed before taking into account in the conceptual model.
- *Reaction parameters:* The predictive simulations were performed by strictly using the rate laws and the associated rate coefficients from the literature values. Although the rate laws of the common minerals (e.g. pyrite, pyrrhotite, or calcite) are somewhat established and they have been extensively studied in the literature under different conditions, a few of the minerals' (e.g. silicates) kinetics were less rigorously explored. Moreover, the literature values of both the rate coefficients and reaction orders for some specific mineral are sometimes found to be varied in a wide range (e.g. Palandri & Kharaka 2004, Declercq & Oelkers 2014). In fact, different investigators often 'arbitrarily' adopt different values for the same minerals in order to match the measured profiles. The exact procedure and common practices to systematically select those reaction parameters are somewhat artificial. As also pointed out in the simulation results, these kinetic parameters have a significant impact on the overall drainage water quality. Therefore, site-specific accurate information regarding the kinetic parameters are crucial to minimise the uncertainties in the predictions.
- *Microbial processes:* The current simulations completely ignored the biological processes that may possibly occur in the waste facilities. In particular, microbial activities can lead to additional oxidation pathways of sulphide minerals by ferric iron. These microbially mediated non-oxidative reaction pathways are generally several orders of magnitude faster than the typical oxidative reaction mechanisms. Presence of such mechanisms may completely alter the predictions of the drainage chemistry. However, extent of such microbial activities must be experimentally confirmed in order to be effectively used in the models.
- *Retardation and sorption like processes:* The presented simulation results were obtained by ignoring any possible retardation mechanisms of the dissolved species in pore water. In reality, the reactive transport of the dissolved ions in pore water solution can be significantly controlled by the processes like ion-exchange between the solution and the solid matrix. Additionally, the dissolved species as well as protons may also interact with the charged mineral surfaces by forming surface complexes via the surface charges. These mechanisms have the potential to retard the dissolved ions, which may lead to significant delays in the concentration fronts in the drainage water.
- *Seasonal variations:* The predicted results in the above sections solely rely on the constant boundary conditions estimated from the annually averaged parameters (e.g.

recharge rate). However, under natural conditions fluctuations exist both seasonally and diurnally. For instance, recharge condition in real sites occurs as a series of pulses (mass loading of water) rather than a constant input on the top of the simulation domain as used in this study. Such fluctuations in water influx involve e.g. the cycle of drying and wetting of waste materials leading to some levels of uncertainty in the overall mineral weathering and reactive transport processes.

- *Dimensionality:* Modelling was performed in strictly 1-D domains conceptualising the propagation of the reaction fronts along the vertical direction of each waste facility. However, the real waste systems (e.g. waste rock piles or tailings impoundment) are three dimensional and the reactive transport processes occur into multiple directions. For instance, gas supply may also occur from the other directions (e.g. sideways) in addition to the top boundary, or the transverse component of the solute and gas transport may dominate the system behaviour compared to the longitudinal component. Nevertheless, 1-D models can be considered as reasonable descriptions of systems that are relatively homogeneous (i.e. low extent of heterogeneity), free of preferential flow paths or fractures, and/or free of important flux boundaries in the transverse direction.
- *Gas transport:* Gas transport was simulated by considering only the diffusive transport through the domain. Quite obviously, in real waste rock piles or tailings facilities gas transport will also take place due to the convective air flow or barometric pressure gradients. Such flow components usually supply the gases into the waste facility from the sides of a pile. However, under “semi-open conditions”, these convective components perhaps would not make a significant difference in system behaviour because gas diffusion is already few orders of magnitude faster than other involved processes such as aqueous phase transport or sulphide oxidation kinetics. Therefore, diffusion of gas is mostly sufficient to supply the oxygen into the system.
- *Heat transport:* The model did not consider the explicit solution of heat transport equations. Instead, a uniform temperature condition, based on the annual average of the temperature at different study sites, was employed. However, in reality temperature gradients are common in the waste facilities involving sulphide weathering processes. Such gradients are usually driven by both air flow as well as the sulphide oxidation reactions that are typically exothermic.

5 CONCLUDING REMARKS

This report presents a model formulation capable of predicting the quality of drainage water from the waste facilities by simulating reactive transport processes occurring in mining environments. The formulation allows integration of the complex mineral and aqueous phase reaction network with the kinetics of mineral dissolution or redox processes, advective-dipsersive transport of aqueous phase components, and gas transport processes. Based on the measured data, the presented model formulation was used in three different mine sites in order to predict the drainage water quality from the waste piles. The first two examples include the prediction in waste rock piles, while the third exercise concerns the predictive simulations in an unsaturated tailings impoundment. These presented examples and the predictive results can be viewed as representative of not only the existing waste piles in a mine site but also the 'future' proposed waste piles in an early phase of a mine, where the waste facility has not been installed yet. These particular exercises demonstrate the capability of the presented modelling framework as well as illustrate how reactive transport modelling can be effectively used in broadcasting the quality of drainage from a waste facility. Such predictive simulations, in connection with the representative site-specific data, can be valuable tools to quantify the possible future occurrences of acid mine drainage and to perform a robust risk assessment in mining environments. Based on the results of the current study, the major conclusions and the possible guidelines for the improvement of prediction quality are briefly summarised in the following points:

- Prediction in a particular waste facility is only as precise as the conceptual understanding regarding the behaviour of the system under investigation. The future behaviour of a system cannot be predicted without achieving a quantitative understanding of the important processes controlling the system dynamics. Therefore, detailed site-specific data should be collected that are representative of the particular study site to develop a realistic conceptual model. The extent of the collected information should be sufficient to identify at least the key mechanisms for that study site.
- Kinetic rate coefficients of different mineral dissolution-precipitation reactions and the reactive mineral surface area are crucial parameters as they strongly dominate the overall geochemistry of the pore water. These parameters may depend on many factors and it is not always possible to derive universal values applicable to every system. Therefore, these kinetic parameters should be experimentally measured by means of laboratory or field scale testing (e.g. humidity cell tests, column/flow-through tests) to be able to gain insights on the speed of the involved reaction kinetics.
- Heterogeneity is ubiquitous in geological material and it exerts a primary control on the overall system behaviour by inducing local variations of the relevant physical and chemical mechanisms/properties throughout the domain. Unfortunately, the effects of heterogeneity are often overlooked in the investigations focusing on the prediction of the drainage water quality or the mine waste management in general. Sometimes such prediction studies are performed based on a very little information (e.g. single data point) for the whole waste facility without any effort to embed heterogeneity. Such predictive

calculations are surely prone to higher degrees of uncertainty as they do not capture the variability of local processes, hence, the results from these calculations may not be reliable predictions of the actual system. Therefore, more efforts, budget, and systematic approaches should be dedicated in detailed data collection to reasonably characterise the physical and chemical properties at different locations of the waste facility.

- It is a common practice to use upscaled parameters in field scale simulations in order to tackle the discrepancy between the laboratory and field conditions (e.g. Malmström et al. 2000). Accurately capturing the scale dependence of reactive transport processes is arguably the most challenging aspect in numerical simulations (e.g. Steefel et al. 2005). Although the concept of scaling was developed to compensate the differences in operating conditions between the laboratory and field scale experiments, the scaling behaviour of reactive transport processes is actually inherited from the inherent heterogeneities and randomness related to the physical transport and chemical agents manifested through geological material properties. In principle, if the distribution and coupling of all the local physicochemical processes at multiple scales were known in a specific waste pile, the importance of scaling would be somewhat reduced. However, in most cases it would be almost impossible to fully characterise all the details of the local scale processes occurring at different scales. Therefore, approaches based on upscaling or downsaling can be practical to describe the reactive transport processes from a macroscopic view. Nevertheless, when using this scaling approach, the scaling factors should be determined applying a systematic investigation based on experiments.
- For the predictive modelling in a planned waste facility at the early stage of a mine (i.e. where the waste disposal has not started yet), all the detailed data regarding the "proposed" waste pile may not be available at hand. However, information must be collected as much as possible from the baseline study, mine planning schemes, and waste characterisation. In particular, details regarding mineralogical composition of the waste materials, geochemical analysis, acid production/neutralisation potential, leaching properties, and possible transport pathways should be collected among others. More importantly, the results of the predictive calculations at this stage should be treated as a "starting point" of the ultimate predictive analysis rather than the final prediction outcomes. In this kind of early stage prediction studies, a systematic monitoring scheme should be established allowing more detailed data collection over the years in order to continuously update the conceptual model as well as to better constrain the numerical model with more site-specific information. This approach would allow realistically calibrating the model with time, and thus would enhance the accuracy of the predictive calculations in a timely fashion.
- In addition to the prediction of effluent quality, the predictive simulations incorporating reactive transport models can also be used in the design and optimisation of the required monitoring/data collection scheme or the waste facility itself to provide a better management of the disposed wastes. For example, numerical simulations along with the hydrogeological conditions in the vicinity of a mine site, can provide insights on the

best possible location for the construction a waste pile. Moreover, by performing such reactive transport simulations at the early stage of a mine, one can identify the frequency of the data collection, and what necessary parameters should be measured in order to rigorously capture the system behaviour. Following such a systematic approach would not only enhance the prediction accuracy but also provide an efficient framework to better control the waste management.

- Another aspect, often neglected in the studies involving mine wastes, is the measurement of spatial profiles/maps of the different quantities in the domain. For instance, mapping of the quantities like oxygen concentrations, temperatures, pH, or dissolved major ions in the different locations of a waste facility may provide better insights regarding the actual processes and their fluxes in the system. Sometimes, it is even impossible to identify the controlling mechanisms without obtaining the spatial information. Among the presented examples, Kylylahti waste rock pile can be a good example that illustrates the importance of measuring spatial profiles to confirm the system behaviour and to explain the fluctuations in the drainage chemistry. In the investigations associated with the prediction of the mine waste effluent, such characterisation along the spatial dimensions can be carried out, for example, by multi-level sampling at different locations of a waste pile.
- Besides the characterisation of the geochemical properties and processes, emphasis should also be given on the fluid flow and transport processes that are sometimes relatively overlooked in dealing with mine waste management. Although, geochemistry has a significant control on the generation of acid mine drainage, the overall reactive transport behaviour in mine waste systems is driven by the fluxes of different reactants into the system. Therefore, information regarding the distributions of hydraulic and transport conditions (e.g. water saturation, permeability, hydraulic conductivity, seepage velocity) should also be collected in order to develop an accurate conceptual model.

In conclusions, the ultimate quality of drainage water from a specific waste facility is determined by the rather complex interplay between factors including flow topology, liquid-solid interactions, heterogeneity, anisotropy, and geochemical reactions. Therefore, it is only expected that a correct prediction of such complex systems would require quantitative understandings of all the important physicochemical processes and their dependencies on the above mentioned factors at a realistic basis. By combining with the good extent of data, predictive modelling can be a very effective technique to establish better management of mine wastes.

6 REFERENCES

Akcil, A., and Koldas, S. (2006). Acid Mine Drainage (AMD): causes, treatment and case studies. Journal of Cleaner Production 14, 1139–1145.

Allison, J. D., Brown, D. S. & Novo-Gradac, K. J. 1991. MINTEQA2/PRODEFA2, A Geochemical Assessment Model for Environmental Systems – Version 3.0 User's Manual. U.S. Environmental Protection Agency Report EPA/600/3-91/021. 106 p.

Alpers, C. N. & Nordstrom, D. K. 1999. Geochemical modelling of water–rock interactions in mining environments. In: Plumlee, G. S. & Logsdon, M. J. (eds) The Environmental Geochemistry of Mineral Deposits, Reviews in Economic Geology, vol. 6A, pp. 289–323. Littleton, CO: Society of Economic Geologists Inc.

AMIRA 2002. ARD Test Handbook. Project P387A Prediction & Kinetic Control of Acid Mine Drainage. AMIRA international, May 2002, 42 p.

Amos, R. T., Blowes, D. W., Bailey, B. L., Sego, D. C., Leslie, S. & Ritchie, I. A. M. 2015. Waste-rock hydrogeology and geochemistry. Applied Geochemistry 57, 140–156.

Amos, R. T. & Mayer, K. U. 2006. Investigating ebullition in a sand column using dissolved gas analysis and reactive transport modelling. Environmental Science & Technology 40, 5361–5367. http://dx.doi.org/10.1016/j.apgeochem.2014.06.020

Appelo, C. A. J. & Postma, D. 2005. Geochemistry, Groundwater and Pollution, second edition, Rotterdam: A. A. Balkema. 649 p.

Appelo, C. A. J. & Wersin, P. 2007. Multicomponent diffusion modeling in clay systems with application to the diffusion of tritium, iodide, and sodium in Opalinus Clay. Environmental Science & Technology 41, 5002–5007.

Archie, G.E. 1942. The electrical resistivity log as an aid in determining some reservoir characteristics. Transactions of the Metallurgical Society of AIME 146.

ASTM 2013. Standard Test Method for Laboratory Weathering of Solid Materials Using a Humidity Cell. ASTM D5744-13.

Ball, J. W., Nordstrom, D. K. & Zachman, D. W. 1987. WATEQ4F – A Personal Computer FORTRAN Translation of the Geochemical Model WATEQ2 with Revised Data Base. U.S. Geological Survey Open-File Report 87-50. 108 p.

Barry, D. A., Prommer, H., Miller, C. T., Engesgaard, P., Brun, A. & Zheng, C. 2002. Modelling the fate of oxidisable organic contaminants in groundwater. Advances in Water Resources 25, 945–983. http://dx.doi.org/10.1016/S0309-1708(02)0 0 044-1

Bigham, J.M., & Nordstrom, D.K. 2000. Iron and Aluminum Hydroxysulfates from Acid Sulfate Waters. Reviews in Mineralogy & Geochemistry 40, 351–403.

Ben-Yaakov S. (1972) Diffusion of sea water ions—I. Diffusion of sea water into a dilute solution. Geochimica et Cosmochimica Acta 36,1395–1406.

Bethke, C. 1997. Modelling transport in reacting geochemical systems. Comptes Rendus de l'Académie des Sciences 324, 513–528.

Blowes, D. W. & Jambor, J. L. 1990. The pore-water geochemistry and the mineralogy of the vadose zone of sulfide tailings, Waite Amulet, Quebec, Canada. Applied Geochemistry 5, 327–346.

Blowes, D. W. & Ptacek, C. J. 1994. Acid-neutralization Mechanisms in Inactive Mine Tailings. In: Jambor, J. L. & Blowes, D. W. (eds) The Environmental Geochemistry of Sulfide Mine Wastes. Mineralogical Association of Canada, Short Course Series, Vol. 31, 95–116.

Blowes, D.W., Ptacek, C.J., Jambor, J.L., & Weisener, C.G. 2003. The Geochemistry of Acid Mine Drainage. In: Holland, H. D. & Turekian, K. K. (eds) Treatise on Geochemistry, (Elsevier), pp. 149–204.

Blowes, D. W., Ptacek, C. J., Jambor, J .L., Weisener, C. G., Paktunc, D., Gould, W. D. & Johnson, D. B. 2014. The Geochemistry of Acid Mine Drainage. In: Holland, H. D. & Turekian, K. K. (eds) Treatise on Geochemistry (Second Edition), Volume 11, 131-190, Elsevier Oxford, ISBN 9780080983004, https://doi.org/10.1016/B978-0-08-095975-7.00905-0.

Blowes, D. W., Smith, L., Sego, D., Smith, L., Neuner, M., Gupton, M., Moncur, M., Moore, M., Klassen, R., Deans, T., Ptacek, C., Garvie, A. & Reinson, J. 2007. Prediction of effluent water quality from waste rock piles in a continuous permafrost region. In: Cidu, R. & Frau, F. (eds) IMWA Symposium 2007: Water in Mining Environments. 27th- 31st May 2007, Cagliari, Italy, 3-9. https://www.imwa.info/docs/imwa_2007/IMWA2007_Blowes.pdf

Boliden 2014. Acquisition of mine and exploration rights in Finland. Power Point presentation, 8.7.2014. Retrieved January 24, 2018. Available at: http://investors.boliden.com/sites/default/files/event/boliden_kylylahti_presentation.pdf

Boudreau B. P., Meysman F. J. R. & Middelburg J. J. 2004 Multicomponent ionic diffusion in porewaters: coulombic effects revisited. Earth & Planetary Science Letters 222, 653–666.

Briggs, P. H. & Meier, A .L. 2002. The determination of forty-two elements in geological materials by inductively coupled plasma-mass spectrometry. In: Taggart, J.E Jr. (Ed.) Analytical methods for chemical analysis of geologic and other materials, U.S. Geological Survey. U.S. Department of the Interior, U.S. Geological Survey. Open-File Report 02-223. Chapter I. https://pubs.usgs.gov/of/2002/ofr-02-0223/I20NAWQAPlus_M.pdf Accessed 7th February 2017.

CEN 2011. CEN/EN 15875. Characterization Of Waste - Static Test For Determination Of Acid Potential Of Sulfidic Waste. European Committee for Standardization, Technical Report, October 2011. 25 p.

Charles, J., Declercq, J., Bowell, R., Barnes, A. & Warrender, R. 2016. Prediction of Source Term Leachate Quality from Waste Rock Dumps: A Case Study from an Iron Ore Deposit in Northern Sweden. In: Drebenstedt, C. & Paul, M. IMWA 2016 – Mining Meets Water – Conflicts and Solutions. Freiberg, Germany, 1170–1174.

Charlton, S. R. & Parkhurst, D. L. 2011. Modules based on the geochemical model PHREEQC for use in scripting and programming languages. Computers & Geosciences 37, 1653–1663. http://dx.doi.org/10.1016/j.cageo.2011.02.005

Criss, J. W. & Birks, L. S. 1968. Calculation methods for fluorescent x-ray spectrometry. Empirical coefficients versus fundamental parameters. Analytical Chemistry 40, 1080–1086.

Crock, J. G., Arbogast, B. F. & Lamothe, P. J. 1999. Laboratory methods for the analysis of environmental samples. In: Plumlee, G. S. & Logsdon, M. J. The Environmental Geochemistry of Mineral Deposits. Littleton, CO: Society of Economic Geologists, 265–288.

Cussler E. L. 2009. Diffusion: Mass Transfer in Fluid Systems, third ed. Cambridge University Press, New York, USA.

Davis, A. & Ashenberg, D. 1989. The aqueous geochemistry of the Berkeley Pit, Butte, Montana, USA. Applied Geochemistry 4, 23–36.

Davis T. & Duff I. 1997. An unsymmetric-pattern multifrontal method for sparse LU factorization. SIAM Journal on Matrix Analysis and Applications 18, 140–158, doi:10.1137/S0895479894246905.

da Silva, J. C., Vargas Jr., E. D. A. & Sracek, O. 2009. Modelling multiphase reactive transport in a waste rock pile with convective oxygen supply. Vadose Zone Journal 8, 1038–1050.

Declercq, J., Charles, J., Bowell, R., Warrender, R & Barnes, A. 2017. Comparison of thermodynamic equilibrium and kinetic approach in the predictive evaluation of waste rock seepage quality in Northern Finland. In: Wolkersdorfer, C., Sartz, L., Sillanpää, M. & Häkkinen, A. (eds) Proceedings, IMWA 2017, Mine Water and Circular Economy. Lappeenranta, Finland 2017, 664–671.

Declercq, J. & Oelkers, E.H. 2014. CarbFix Report 4 PHREEQC mineral dissolution kinetics database. CarbFix Project no. 281348. Geoscience Environement Toulouse, Belin, Toulouse. https://www.or.is/sites/or.is/files/kinetic_database.pdf

Dold, B. 2017. Acid rock drainage prediction: A critical review. Journal of Geochemical Exploration 172, 120–132.

Dold, B. 2003. Speciation of the most soluble phases in a sequential extraction procedure adapted for geochemical studies of copper sulfide mine waste. Journal of Geochemical Exploration 80, 55–68.

Dold, B. 2010. Basic concepts in environmental geochemistry of sulfidic mine-waste management. In: Kumar, S. E. (ed.) Waste Management, InTech, 173-198. DOI: 10.5772/8458. https://www.intechopen.com/books/waste-management/basic-concepts-in-environmental-geochemistry-of-sulfidic-mine-waste-management

Doležal, J., Provondra, P. & Šulcek, Z. 1968. Decomposition techniques in inorganic analysis. Iliffe Books Ltd, London. 224 p.

Domènech, C., de Pablo, J., & Ayora, C. 2002. Oxidative dissolution of pyritic sludge from the 3098 Aznalcollar mine (SW Spain). Chemical Geology 190, 339–353.

Eary, L. E., Runnells D. D. & Esposito, K. J. 2003. Geochemical controls on ground water composition at the Cripple Creek Mining District, Cripple Creek, Colorado. Applied Geochemistry 18, 1–24.

Eriksson, N., Gupta, A., & Destouni, G. 1997. Comparative analysis of laboratory and field tracer tests for investigating preferential flow and transport in mining waste rock. Journal of Hydrology 194, 143–163.

Fala, O., Molson, J., Aubertin, M., Bussière, B., 2005. Numerical modelling of flow and capillary barrier effects in unsaturated waste rock piles. Mine Water Environment 24, 172–185.

Fala, O., Molson, J., Aubertin, M., Dawood, I., Bussière, B. & Chapuis, R. P. 2013. A numerical modelling approach to assess long-term unsaturated flow and geochemical transport in a waste rock pile. International Journal of Mining, Reclamation and Environment 27(1), 38–55.

GTK 2018. Kylylahti. Mineral Deposit Report database. Retrieved April 28, 2018. Available at: http://tupa.gtk.fi/karttasovellus/mdae/raportti/112_Kylylahti.pdf

Gunsinger, M. R., Ptacek, C. J., Blowes, D. W., Jambor, J. L. & Moncur, M. C. 2006. Mechanisms controlling acid neutralization and metal mobility within a Ni-rich tailings impoundment. Applied Geochemistry 21, 1301–1321.

Hansen, J. B., Holm, P. E., Hansen, E. A. & Hjelmar, O. 2000. Use of lysimeters for characterization of leaching from soil and mainly inorganic waste materials. Nordtest Technical Report 473. 49 p.

He, W., Beyer, C., Fleckenstein, J. H., Jang, E., Kolditz, O., Naumov, D. & Kalbacher, T. 2015. A parallelization scheme to simulate reactive transport in the subsurface environment with OGS#IPhreeqc 5.5.7-3.1.2. Geoscientific Model Development 8, 3333–3348. http://dx.doi.org/10.5194/gmd- 8- 3333–2015

Heikkinen, P. M. & Räisänen, M. L. 2009. Trace metal and As solid-phase speciation in sulphide mine tailings – Indicators of spatial distribution of sulphide oxidation in active tailings impoundments. Applied Geochemistry 24, 1224–1237.

INAP 2009. The GARD Guide. The Global Acid Rock Drainage Guide (GARD Guide). The International Network for Acid Prevention (INAP). http://www.gardguide.com/

Jambor, J. L. 2003. Mine-waste mineralogy and mineralogical perspectives of acid-base accounting. In: Jambor, J. L., Blowes, D. W. & Ritchie, A. I. M. (eds). Environmental Aspects of Mine Wastes. Ottawa, Ontario: Mineralogical Association of Canada, 117–146.

Jambor, J. L., & Owens, D. R. 1993. Mineralogy of the tailings impoundment at the former Cu-Ni deposit of Nickel Rim Mines Ltd., eastern edge of the Sudbury structure, Ontario, Technical Report MSL 93-4, Mineralogical Science Laboratory Division, Ottawa, Ontario, Canada, 1993.

Javadi, M., Peterson, H.E., Blackmore, S.R., Mayer, K.U., Beckie, R.D., & Smith, L., 2012. Evaluating preferential flow in an experimental waste rock pile using unsaturated flow and solute transport modeling. In: Proceedings International Conference on Acid Rock Drainage (ICARD) Ottawa, 9th, Canada, 20–26 May, 2012.

Johnson, D.B., & Hallberg, K.B. 2005. Acid mine drainage remediation options: a review. Science of Total Environment 338, 3–14.

Karlsson, T., Kauppila, P. M., Lehtonen, M., Tiljander, M., Forsman, P. & Lahtinen, T. 2018. Laboratorioanalyysit kaivannaisjätteiden käyttäytymisen ennustamisessa. Geologian tutkimuskeskus, Työraportti 13/2018. (In Finnish)

Kontinen, A., Peltonen, P. & Huhma, H. 2006. Description and genetic modelling of the Outokumpu-type rock assemblage and assiciated sulphide deposits. GTK report M 10.4/2006/1. 380 p. http://tupa.gtk.fi/raportti/arkisto/m10_4_2006_1.pdf

Korrani, A. K. N., Sepehrnoori, K. & Delshad, M., 2015. Coupling IPhreeqc with UTCHEM to model reactive flow and transport. Computers & Geosciences 82, 152–169. http://dx.doi.org/10.1016/j.cageo.2015.06.004

Kylylahti Copper Oy 2006. Kylylahden kaivos – Ympäristövaikutusten arviointiselostus. 31.5.2006. 128 p. (in Finnish) http://www.ymparisto.fi/download/noname/%7B43D09F46-7C8F-4204-A31C-2E9612B2293A%7D/41608

Lahmira, B. & Lefebvre, R. 2014. Numerical modelling of transfer processes in a waste rock pile undergoing the temporal evolution of its heterogeneous material properties. International Journal of Mining, Reclamation and Environment, 29(6), 499–520.

Lahmira, B., Lefebvre, R., Aubertin, M. & Bussière, B. 2016. Effect of heterogeneity and anisotropy related to the construction method on transfer processes in waste rock piles. Journal of Contaminant Hygrology 184, 35–49.

Lasaga, A. C. 1979. The treatment of multi-component diffusion and ion pairs in diagenetic fluxes. American Journal of Science 279, 324–346.

Lawrence, R. W. & Wang, Y. 1997. Determination of Neutralization Potential in the Prediction of Acid Rock Drainage. In: Fourth International Conference on Acid Rock Drainage, Vancouver, B.C. May 31-June 6, 1996. Proceedings, Volume I, 449–464

Lefebvre, R., Hockley, D., Smolensky, J. & Lamontagne, A. 2001. Multiphase transfer processes in waste rock piles producing acid mine drainage 2: Applications of numerical simulation. Journal of Contaminant Hydrology 52, 165–186.

Levenspiel, O. 1972. Chemical Reaction Engineering. Second edition. New York: John Wiley and Sons. 578 p.

Linklater, C. M., Sinclair, D. J. & Brown, P. L. 2005. Coupled chemistry and transport modelling of sulphidic waste rock dumps at the Aitik mine site, Sweden. Applied Geochemistry 20, 275–293.

Lottermoser, B. 2010. Mine Wastes: Characterization, Treatment, Environmental Impacts. Springer-Verlag Berlin, Heidelberg.

Maest, A. & Nordstrom, K. 2017. A geochemical examination of humidity cell tests. Applied Geochemistry 81, 109–131.

Maest, A. S., Kuipers, J. R., Travers, C. L., & Atkins, D. A. 2005. Predicting Water Quality at Hardrock Mines: Methods and Models, Uncertainties, and State-of-the-Art. Kuipers & Associates and Buka Environmental. 77 p. http://www.ceaa-acee.gc.ca/050/documents_staticpost/cearref_3394/hearings/SM09.pdf

Makkonen H. & Halkoaho T. 2007. Whole rock analytical data (XRF, REE, PGE) for several Svecofennian (1.9 Ga) and Archean (2.8 Ga) nickel deposits in eastern Finland. Geological Survey of Finland, Archive report, M19/3241/2007/32. 49p. Available at: http://tupa.gtk.fi/raportti/arkisto/m19_3241_2007_32.pdf

Makkonen, H. 2015. Nickel Deposits of the 1.88 Ga Kotalahti and Vammala Belts. In: Maier, W.D., Lahtinen, R. & O'Brien, H. (Eds.) 2015. Mineral Deposits of Finland, Chapter 3.8. Elsevier, 802 p.

Malmström, M. E., Destouni, G., Banwart, S. A. & Stromberg, B. 2000. Resolving the scale-dependence of mineral weathering rates. Environmental Science and Technology 34, 1375–1378.

Mayer, K. U., Alt-Epping, P., Jacques, D., Arora, B. & Steefel, C. I. 2015. Benchmark problems for reactive transport modelling of the generation and attenuation of acid rock drainage. Computers & Geosciences 19, 635–653. doi:10.1007/s10596-015-9476-9

Mayer, K. U., Blowes, D. W. & Frind, E. O. 2003. Advances in reactive-transport modelling of contaminant release and attenuation from mine-waste deposits. In: Jambor J. L., Blowes D. W. & Ritchie A .I. M. (eds.) Environmental aspects of mine wastes. Mineralogical Association of Canada Short Course Series 31, 283–302. Ottawa: Mineralogical Association of Canada.

Mayer, K. U., Frind, E. O. & Blowes, D. W. 2002. Multicomponent reactive transport modelling in variably saturated porous media using a generalized formulation for kinetically controlled reactions. Water Resources Research 38, 1174–1195.

MEND 2012. Cold regions cover system design technical guidance document. MEND report 1.61.5c, July 2012. 135 p. http://mend-nedem.org/wp-content/uploads/2013/01/1.61.5c.pdf

MEND 2017. Reports, prediction. http://mend-nedem.org/category/prediction/

Molson, J. W., Fala, O. Aubertin, M. & Bussière, B. 2005. Numerical simulations of pyrite oxidation and acid mine drainage in unsaturated waste rock piles. Journal on Contaminant Hydrology 78, 343–371.

Miller, S. D., Jeffery, J. J. & Murray, G. S. C. 1990. Identification and management of acid generating mine wastes – Procedures and practices in Southeast Asia and the Pacific Regions. In: Gadsby, J. W., Malick, J. A. & Day S. J. (eds) Acid Mine Drainage Designing for Closure, BiTech Publishers Ltd. Vancouver, B.C., 1–11.

Millington, R. J. 1959. Gas diffusion in porous media, Science, 130, 100– 102.

Moncur, M. C., Ptacek, C. J., Blowes, D. W. & Jambor, J. L. 2005. Release, transport and attenuation of metals from an old tailings impoundment. Applied Geochemistry 20, 639–659.

Morin, K. A. & Hutt, N. M. 1994. An empirical technique for predicting the chemistry of water seeping from mine-rock piles. In: Proceedings, America Society of Mining and Reclamation,

1993, 12–19. http://www.asmr.us/Portals/0/Documents/Conference-Proceedings/1994-Volume-1/0012-Morin.pdf. Accessed 4th July 2017.

Morin, K. A. & Hutt, N. M. 1999. Internet Case Study #10: Comparison of NAG Results to ABA Results for the Prediction of Acidic Drainage. Minesite Drainage Assessment Group (MDAG). http://www.mdag.com/case_studies/cs1-99.html

Muniruzzaman, M., Haberer, C. M., Grathwohl, P. & Rolle, M. 2014. Multicomponent ionic dispersion during transport of electrolytes in heterogeneous porous media: Experiments and model-based interpretation. Geochimica et Cosmochimica Acta 141, 656–669.

Muniruzzaman, M., Kauppila, P. M. & Karlsson, T. 2018. Water quality prediction of mining waste facilities based on predictive models. Geological Survey of Finland, Open File Research Report 16/2018. 65 p

Muniruzzaman, M. & Rolle, M. 2016. Modelling multicomponent ionic transport in groundwater with IPhreeqc coupling: Electrostatic interactions and geochemical reactions in homogeneous and heterogeneous domains. Advances in Water Resources 98, 1–15. doi:10.1016/j.advwatres.2016.10.013

Müller, M., Parkhurst, D. L. & Charlton, S. R. 2011. Programming PHREEQC calculations with C ++ and Python - a comparative study. In: Maxwell, R., Poeter, E., Hill, M. & Zheng, C. (eds) MODFLOW and More 2011: Integrated Hydrological Modeling – Conference Proceedings, 632–636.

Nagy, K. L. 1995. Dissolution and precipitation kinetics of sheet silicates, in Chemical Weathering Rates of Silicate Minerals, Reviews in Mineralogy 31,173– 233.

Nardi, A., Idiart, A., Trinchero, P., de Vries, L. M. & Molinero, J. 2014. Interface COMSOL-PHREEQC (iCP), an efficient numerical framework for the solution of coupled multiphysics and geochemistry. Computers & Geosciences 69, 10–21. http://dx.doi.org/10.1016/j.cageo.2014.04.011

Nasir, O., Fall, M. & Evgin, E. 2014. A simulator for modelling of porosity and permeability changes in near field sedimentary host rocks for nuclear waste under climate change influences. Tunneling and Underground Space Technology 42, 122–135. http://dx.doi.org/10.1016/j.tust.2014.02.010

Neuman, S. P. 1973. Saturated-unsaturated seepage by finite elements, Journal of the Hydraulics Division - Civil Engineering Database 99(HY12), 2233–2250.

Nordstrom, D.K., & Alpers, C.N. 1999. Geochemistry of acid mine waters. Reviews in Economic Geolology 6, 133–160.

Nordstrom D. K. & Campbell, K. M. 2014. Modelling Low-Temperature Geochemical Processes. In: Holland, H. D. & Turekian, K. K. (eds) Treatise on Geochemistry, Second Edition, Vol. 7, pp. 27–68.

Nordstrom D. K. & Munoz, J. L. 1994. Geochemical Thermodynamics. Oxford: Blackwell Scientific Publications. 493 p.

Nordstrom, D. K. & Nicholson A. 2017 (eds). Geochemical Modeling for Mine Site Characterization and Remediation. Society for Mining, Metallurgy & Exploration, Colorado, USA, 181 p.

Nordstrom, D. K., Alpers, C. N., Ptacek, C. J. & Blowes, D. W. 2000. Negative pH and extremely acidic mine waters from Iron Mountain, California. Environmental Science & Technology 34, 254–258.

Nordstrom, D. K, Blowes, D. W. & Ptacek, C. J. 2015. Hydrogeochemistry and microbiology of mine drainage: An update. Applied Geochemistry 57, 3–16. https://doi.org/10.1016/j.apgeochem.2015.02.008

Pabst, T., Molson, J., Aubertin, M. & Bussiere, B. 2017. Reactive transport modelling of the hydro-geochemical behaviour of partially oxidized acid-generating mine tailings with a monolayer cover. Applied Geochemistry 78, 219–233.

Palandri, J.L., & Kharaka, Y.K., 2004. A compilation of rate parameters of water-mineral interaction kinetics for application to geochemical modeling: USGS Open File Report 2004-1068, Menlo Park, California, National Energy Technology Laboratory – United States Department of Energy.

Pantelis, G. 1993. FIDHELM: Description of Model and Users Guide. Australian Nuclear Science and Technology Organization Report, ANSTO/M123.

Parbhakar-Fox, A. & Lottermoser, B. G. 2015. A critical review of acid rock drainage prediction methods and practices. Minerals Engineering 82, 197–124.

Parkhurst, D. L. & Appelo, C. A. J. 2013. Description of input and examples for PHREEQC version 3 – a computer program for speciation, batch-reaction, one dimensional transport, and inverse geochemical calculations. U.S. Geological Survey Techniques and Methods 6-A43:497. http://pubs.usgs.gov/tm/06/ a43/ Accessed 5th June 2017.

Parkhurst, D. L., Kipp, K. L., Engesgaard, P. & Charlton, S. R. 2005. PHAST - A program for simulating ground-water flow, solute transport, and multicomponent geochemical reactions. U.S. Geological Survey Techniques and Methods 6–A35. 235 p.

Parkhurst, D. L., Thorstenson, D. C., & Plummer, L. N. 1985. PHREEQE – A computer program for geochemical calculations. U.S. Geological Survey Water Resources Investigations Report 80–96. 195 p.

Pedretti, D., Mayer, K. U. & Beckie, R. D. 2017. Stochastic multicomponent reactive transport analysis of low quality drainage release from waste rock piles: Controls of the spatial distribution of acid generating and neutralizing minerals. Journal of Contaminant Hydrology 201, 30–38. https://doi.org/10.1016/j.jconhyd.2017.04.004

Plumlee, G.S. 1999. The environmental geology of mineral deposits. Reviews in Economic Geology 6A, 71–116.

Plummer, L.N., Wigley, T. M. L., & Parkhurst, D.L. 1978.The kinetics of calcite dissolution in CO_2 -water systems at 5 degrees to 60 degrees C and 0.0 to 1.0 atm CO_2. American Journal of Science 278, 179-216.

Pohjois-Suomen AVI 2007. Pyhäsalmen kaivoksen ympäristö- ja vesitalouslupa, Pyhäjärvi. Lupapäätös 85/07/02. 70 p. (in Finnish). Available at: http://www.ymparisto.fi/download/noname/%7B894B5FE1-3E1C-4223-A0CC-08BC68BF9A60%7D/86841

Price, W. A. 2009. Prediction Manual for Drainage Chemistry from Sulfidic Geologic Materials. Natural Resources Canada. MEND Report 1.20.1. 579 p.

Price, W. A., Morin, K. & Hutt, N. 1997. Guidelines for the prediction of acid rock drainage and metal leaching for mines in British Columbia: Part II. Recommended procedures for static and kinetic tests. In: Fourth International Conference on Acid Rock Drainage, Vancouver, B.C. May 31 - June 6, 1996. Proceedings, volume 1, 15–30. http://www.mdag.com/MDAG%20Paper%20Database/M0036%20-%20Price%20et%20al%201997%20-%20BC%20Government%20Guidelines.PDF Accessed 5.6.2017

Ramstedt, M., Carlsson, E. & Lövgren, L. 2003. Aqueous geochemistry in the Udden pit lake, Northern Sweden. Applied Geochemistry 18, 97–108.

Reimann, C., Caritat, P.D., Halleraker, J.H., Volden, T., Äyräs, M., Niskavaara, H., Chekushin, V.A., Pavlov, V.A. 1997. Rainwater composition in eight arctic catchments in northern Europe (Finland, Norway and Russia). Atmospheric Environment 31(2), 159-170, ISSN 1352-2310. https://doi.org/10.1016/1352-2310(96)00197-5.

Reynolds, R. C. 1989. Principles of Powder Diffraction. In: Bish, D. L & Post, J. E. (eds) Modern Powder Diffraction, Mineralogical Society of America, Reviews in Mineralogy, Vol. 20, 1–18.

Rimstidt, J.D., & Barnes, H.L. 1980. The kinetics of silica-water reactions. Geochimica et Cosmochimica Acta 44(11), 1683-1699, ISSN 0016-7037. https://doi.org/10.1016/0016-7037(80)90220-3.

Rimstidt, J.D., & Vaughan, D.J. 2003. Pyrite oxidation: a state-of-the-art assessment of the reaction mechanism. Geochimica et Cosmochimica Acta 67, 873–880.

Rolle, M., Muniruzzaman, M., Haberer, C. M. & Grathwohl, P. 2013. Coulombic effects in advection-dominated transport of electrolytes in porous media: multicomponent ionic dispersion. Geochimica et Cosmochimica Acta 120, 195–205.

Sapsford, D. J., Bowell, R. J., Dye, M. & Williams, K. P. 2009. Humidity cell test for the prediction of acid rock drainage. Minerals Engineering 22(1), 25–36.

Shokri, B. J., Ardejani, F. D., Ramazi, H. & Moradzadeh, A. 2016. Predicting pyrite oxidation and multi-component reactive transport processes from an abandoned coal waste pile by comparing 2D numerical modeling and 3D geo-electrical inversion. International Journal of Coal Geology 164, 13–24.

Scheidegger, A.E., 1961. General theory of dispersion in porous media. Journal of Geophysical Research 66, 3273–3278. http://dx.doi.org/10.1029/JZ066i010p03273 .

Šimunek, J., Jacques, D., Šejna, M. & Van Genuchten, M. T. 2012. The HP2 program for HYDRUS (2D/3D): A coupled code for simulating two-dimensional variably-saturated water

flow, heat transport, and biogeochemistry in porous media. In: Version 1.0. PC Progress, Prague, Czech Republic. 76 p.

Sobek, A., Schuller, W., Freemen, J. & Smith, R. 1978. Field and Laboratory Methods Applicable to Overburdens and Minesoils. Industrial Environmental Research Laboratory, Office of Research and Development, U.S. Environmental Protection Agency, Cincinnati, Ohio. Environmental Protection Technology Series, Report EPA-600/2-78-054. 216 p.

Steefel, C. I. & Lasaga, A. C. 1994. A coupled model for transport of multiple chemical species and kinetic precipitation dissolution reactions with application to reactive flow in single-phase hydrothermal systems. American Journal of Science 294, 529–592.

Steefel, C.I., DePaolo, D.J. & Lichtner, P.C. 2005. Reactive transport modeling: An essential tool and a new research approach for the Earth sciences. Earth and Planetary Science Letters 240(3–4), 539-558, ISSN 0012-821X, https://doi.org/10.1016/j.epsl.2005.09.017.

Steefel, C. I., Appelo, C. A. J., Arora, B., Jacques, D., Kalbacher, T., Kolditz, O. & Yeh, G. T. 2015a. Reactive transport codes for subsurface environmental simulation. Computational Geosciences 19, 445–78. doi: 10.1007/s10596-014-9443-x

Tempel, R. G., Shevenell, L. A., Lechler, P. & Price, J. 2000. Geochemical modelling approach to predicting arsenic concentrations in a mine pit lake. Applied Geochemistry 15, 475–492.

Tornivaara, A., Räiusänen, M. L., Kovalainen, H. & Kauppi, S. 2017. Suljettujen ja hylättyjen kaivosten kaivannaisjätealueiden jatkokartoitus (KAJAKII). Loppuraportin luonnos 16.10.2017. 144p. (in Finnish).

Tripathy, D.P. 2014. Prevention and Treatment of Acid Mine Drainage: An Overview. In Sengupta, D. (ed.), Recent Trends in Modelling of Environmental Contaminants 95–117, DOI 10.1007/978-81-322-1783-1_4, Springer India 2014.

Tremblay, G. A. & Hogan, C. M. 2000. MEND Manual, Volume 3 – Prediction. Natural Resources Canada. MEND Report 5.4.2c. 105 p.

White, W. W. III, Trujillo, E. M. & Lin, C.-K.1994. Chemical predictive modelling of acid mine drainage from waste rock: model development and comparison of modelled output to experimental data. Paper presented at International Land Reclamation and Mine Drainage Conference and the Third International Conference on the Abatement of Acidic Drainage, Pittsburgh, PA, USA, April 24–29 1994. http://www.asmr.us/Portals/0/Documents/Conference-Proceedings/1994-Volume-1/0157-White.pdf

White, W. W. III, Lapakko, K. A. & Cox, R. L. 1999. Static-test methods most commonly used to predict acid mine drainage: Practical Guidelines for Use and Interpretation. In: Plumlee, G.S. & Logsdon, M. (eds) The Environmental Geochemistry of Mineral Deposits, Part A: Theory and background. Society of Economic Geologists, Reviews in Economic Geology, vol. 7A, 325–338.

Williams, R. D. & Diehl, S. F. (eds) 2014. Techniques for Predicting Metal Mining Influenced Water. Management Technologies for Metal Mining Influenced Water, Vol. 5. Englewood, CO: SME. 250 p.

Williamson, M. A. & Rimstidt, J. D. 1994. The kinetics and electrochemical rate-determining step of aqueous pyrite oxidation. Geochimica et Cosmochimica Acta 58, 5443–5454.

Wissmeier, L. & Barry, D. A. 2011. Simulation tool for variably saturated flow with comprehensive geochemical reactions in two- and three-dimensional domains. Environmental Modelling & Software 26, 210–218. http://dx.doi.org/10.1016/j.envsoft.2010.07.005

Wolery, T. J. 1992. EQ3/6 – A Software Package for Geochemical Modelling of Aqueous Systems. Lawrence Livermore National Laboratory, CA.

Wösten, J. H. M. & van Genuchten, M. T. 1988. Using texture and other soil properties to predict the unsaturated soil hydraulic functions, Soil Science Society of America Journal, 52, 1762–1770, 1988.

Wunderly, M. D., Blowes, D. W., Frind, E. O. & Ptacek, C. J. 1996. A multicomponent reactive transport model incorporating kinetically controlled pyrite oxidation. Water Resources Research 32, 3173–3187.

Xu, T. & Pruess, K. 2001. Modelling multiphase non-isothermal fluid flow and reactive geochemical transport in variably saturated fractured rocks 1: methodology. American Journal of Science 301, 16–33. http://dx.doi.org/10.2475/ajs.301.1.16